Greying and Gravity: Population Ageing and the Regional Gains from Integration in China

Chenxin Jin* Wei Jin† Yang Pei‡ Bin Sheng§ Bing Yan¶

Abstract

We study how population ageing changes the regional gains from domestic and external integration in China. We document that: ageing is spatially uneven across provinces, migrants are disproportionately young, and labor income follows a hump-shaped life-cycle profile. These facts motivate a multi-region, multi-sector Ricardian trade model with age-varying labor efficiency, migration elasticities, and migration frictions, in which regions are connected through internal migration, interregional trade, and trade with the rest of the world. Using 2017 as the benchmark, we reset the age structure, domestic migration costs, internal trade costs, and China–rest-of-world trade costs to their 1997 values. Ageing reshapes the gains from integration: under the older age structure, domestic migration integration generates larger real-wage gains, whereas internal and external trade integration generate slightly smaller gains. Provincial results show substantial spatial reallocation, with internal trade integration generating the largest redistribution and external integration favoring more internationally connected regions.

JEL Classification: F11, F43, J11, R12

Keywords: Population ageing; Domestic integration; International trade; Spatial inequality

*APEC Study Center, Nankai University. Email: jinchenxin@nankai.edu.cn.

†School of Economics, Nankai University. Email: wei.jin.economics@gmail.com.

‡Institute of Energy, Environment, and Economy, Tsinghua University. Email: ypei1.work@gmail.com.

§School of Economics, Nankai University. Email: shengbin@nankai.edu.cn.

¶School of Economics, Nankai University. Email: yanbing@nankai.edu.cn.

1 Introduction

China's economic growth has long been supported by a large working-age population, extensive internal migration, deepening domestic market integration, and increasing openness to world markets. This environment is changing. India overtook China as the world's most populous country in 2023, and China entered a phase of negative natural population growth in 2022, when deaths exceeded births. At the same time, external integration has faced new uncertainty, especially after the U.S.–China trade war and the broader rise of geopolitical frictions. These demographic and external changes raise concerns about whether the forces that supported China's past growth can continue to generate broad-based gains across regions.

Policy responses have placed renewed emphasis on domestic adjustment. Hukou reforms aim to lower migration barriers and improve the spatial allocation of labor, while the dual-circulation strategy emphasizes domestic demand, internal market integration, and the resilience of China's economic structure. Yet the welfare and distributional effects of these forces remain difficult to assess separately. Population ageing, lower domestic migration costs, lower internal trade costs, and changes in China–ROW trade costs all affect aggregate income and regional inequality, but they operate through different channels and may interact with one another. This paper therefore asks: How do population ageing, domestic migration integration, internal trade integration, and external trade integration affect China's aggregate welfare and regional income distribution? How much does each force contribute to income changes? And how does population ageing reshape the gains from domestic and external integration?

This paper quantifies how population ageing changes the aggregate and regional gains from domestic and external integration in China. We begin by documenting three facts: ageing is spatially uneven across provinces, migrants are disproportionately young, and labor income follows a hump-shaped life-cycle profile. These facts imply that age structure matters for both effective labor supply and spatial labor reallocation. We then embed age heterogeneity into a multi-region, multi-sector Ricardian trade model in which workers differ by age in labor efficiency, migration elasticities, and migration frictions, while regions are connected through internal migration, interregional trade, and trade with the rest of the world. Calibrating the model to China, we compare the 2017 benchmark economy with counterfactuals that reset the age structure, domestic migration costs, internal trade costs, and China–ROW trade costs to their 1997 values. The results show that ageing directly lowers aggregate real wage income per effective worker and raises regional real-wage inequality. Ageing also changes the gains from integration: under the older age structure, migration frictions become more costly for labor allocation, so domestic migration integration generates larger real-wage gains, whereas internal and external trade integration generate slightly smaller gains. At the provincial level, internal trade integration produces the largest spatial reallocation, external integration benefits more internationally connected regions, and migration integration redistributes gains across origin and destination provinces. These findings show that demographic structure is not only a source of regional inequality, but also a state variable that shapes the welfare and spatial consequences of integration.

Our stylized-fact analysis combines aggregate demographic statistics with population-survey microdata at the individual and provincial levels. We document three key facts. First, China has entered a period of rapid demographic ageing: births declined sharply after 2016, deaths exceeded births in 2022, and negative natural population growth has since widened. Second, ageing is highly uneven across regions. Guangdong's resident population is about seven years younger on average than that of Northeast China, and this regional gap is closely related to age-selective migration: migrants are disproportionately young and concentrated in prime working ages. Third, individual labor income follows a hump-shaped life-cycle profile, rising from young ages to prime working ages and peaking around age 38 before declining at older ages. These patterns suggest that ageing affects regional outcomes not only by changing the size of the workforce, but also by altering the spatial distribution of effective labor through age-specific labor efficiency and migration responses. We next develop a quantitative model to capture these channels.

We then develop a quantitative spatial model of China with age-specific labor mobility, interregional trade, and trade with the rest of the world. The economy consists of Chinese province-level regions and an aggregated rest-of-world region. Workers are mobile across Chinese regions but not internationally, and goods are traded across regions and with the rest of the world subject to sector-specific trade costs. The key features are that provinces have different age distributions, and workers of different ages differ in labor efficiency, migration elasticities, and bilateral migration frictions.

These features imply that ageing affects the economy through two related margins: it changes the regional supply of effective labor, and it changes how strongly workers respond to differences in regional real payoffs. In this environment, lower domestic migration frictions, lower internal trade costs, and lower China–ROW trade costs operate through linked spatial general-equilibrium channels. They change market access, input prices, sectoral prices, and regional real payoffs, reallocating production, consumption, and workers across provinces. These reallocations feed back into effective labor supply, production costs, comparative advantage, and trade patterns. Age structure governs the strength of this feedback: with an older labor force, migration responds less to the same real-payoff changes, so the same integration shock generates different aggregate and spatial gains than it would under a younger age structure.

We calibrate the model to match the benchmark economy. The benchmark economy has 30 mainland province-level regions, excluding Tibet, one rest-of-world region, three sectors, and three working-age groups. The calibration combines population micro data, Chinese provincial MRIO tables, OECD ICIO tables, and Penn World Table data. The 2005 National 1% Population Sample Survey estimates age-specific labor efficiency and migration elasticities. Middle-age workers supply 1.06 efficiency units and old workers 0.92 relative to young workers, while migration elasticities decline from 3.21 to 2.68 and 2.21. These estimates capture the key life-cycle force: workers are most productive in middle age, but mobility responses weaken with age. The 2015 survey provides regional age distributions, participation rates, and migration shares; the remaining data discipline production, input-output linkages, expenditure, trade, imbalances, and China–ROW flows. Productivities, trade costs, and migration frictions are recovered from equilibrium conditions.

The calibration delivers three patterns. First, age heterogeneity is quantitatively important: recovered migration frictions rise from 8.16 for young workers to 11.73 for middle-age workers and 28.53 for old workers. Second, the 2017 benchmark features sizable domestic and external frictions, with China–ROW trade costs exceeding internal trade costs in all sectors. Third, the calibrated 1997-to-2017 shocks show that China became older and more integrated. Relative to 2017, the 1997 economy had a younger age structure and higher migration, internal-trade, and external-trade frictions, with pooled ratios of 1.95, 1.26, and 1.42. The benchmark economy closely reproduces wages, sectoral expenditures, trade shares, and migration shares, providing the basis for the counterfactual analysis.

We use the calibrated model to quantify the role of population ageing in China's regional economy. The counterfactual analysis has two goals: to measure the direct effect of the older age structure on aggregate real wages and spatial inequality, and to examine how ageing changes the gains from domestic and external integration. The 2017 economy is the benchmark. We then reset selected fundamentals to their 1997 calibrated values, holding all other fundamentals at their 2017 levels. These fundamentals include age shares, domestic migration frictions, internal trade costs, and China–ROW trade costs. In the demographic experiment, we reset age shares rather than population levels, so aggregate population is held fixed. In the integration experiments, we reset migration frictions, interregional trade costs, and China–ROW trade costs to their 1997 values, one at a time and in combination. Comparing each counterfactual with the benchmark gives the contribution of the corresponding 1997–2017 change. Comparing these contributions under the 2017 and 1997 age structures then shows how population ageing changes the gains from integration.

We organize the counterfactual results into two parts: aggregate effects and provincial spatial reallocation. The aggregate counterfactuals deliver three main results. First, ageing directly lowers real wage income per effective worker by 0.46 percent and raises regional real-wage inequality by 0.87 percent, holding aggregate population fixed. Second, real-wage gains from integration are concentrated in goods flows: domestic trade integration raises real wages by 7.82 percent, compared with 2.44 percent from domestic migration integration and 3.13 percent from external integration. Third, ageing changes these gains through labor reallocation. Because older workers respond less to migration incentives, lower migration frictions generate larger marginal gains even with weaker migration responses. Ageing raises the gain from domestic migration integration by 6.1 percent, while slightly reducing the gains from domestic trade and external integration.

We then turn to the provincial perspective, which delivers three main results. First, internal trade integration generates the largest spatial reallocation: reversing the 1997–2017 decline in internal trade costs raises real wage income per effective worker by as much as 14.31 percent in some provinces, while lowering it in provinces that benefited more from domestic market integration. Second, external and migration integration have different spatial footprints: reversing external integration lowers real wage income in most provinces, with the largest loss reaching 12.45 percent, while reversing migration integration raises real wage income in some developed destination provinces, with Shanghai increasing by 11.21 percent. Third, ageing changes these provincial effects. Under the 1997 age structure, Shanghai's loss from reversing external integration deepens from 12.45 percent to 14.70 percent, while its gain from reversing migration integration falls from 11.21 percent to 6.06 percent. Thus, the provincial results show that ageing reshapes not only aggregate gains, but also the geography of gains and losses from integration.

This paper relates first to the literature on demographic change and its economic consequences. The closest related paper is Suzuki (2023), who builds a life-cycle spatial model of migration and local shocks in an aging economy. Giannone et al. (2024) uses detailed regional data for Japan to show that youth out-migration drives rural depopulation and aging, with adverse effects on local economic activity. Greenland, Lopresti, and McHenry (2019) and Boustan et al. (2020) provide empirical evidence that younger workers respond more strongly to local shocks than older workers. Related macro work shows that aging slows labor-market dynamism more broadly. For example, Karahan and Rhee (2017) show that U.S. interstate migration fell by about half from the 1980s onward, with population aging accounting for roughly half of the decline. Like these papers, we study how aging affects spatial economic outcomes. We depart from this literature by focusing on China in an open-economy framework, where age-dependent labor efficiency, migration elasticities, and migration frictions jointly shape labor reallocation and the gains from integration.

Second, this paper contributes to the literature on internal integration and the spatial allocation of economic activity. A large body of work studies how geography, trade costs, and labor mobility shape the allocation of production and workers across space. Allen and Arkolakis (2014), Redding (2016), and Ahlfeldt et al. (2015) develop quantitative spatial frameworks in which trade and mobility frictions affect regional activity and welfare. Related work by Caliendo et al. (2018) and Caliendo, Dvorkin, and Parro (2019) shows how productivity and trade shocks propagate across regions through trade linkages, input-output linkages, and worker mobility. In the Chinese context, Young (2000) and Poncet (2003) emphasize domestic market segmentation and measure the extent of provincial market integration. Tombe and Zhu (2019) quantify the aggregate and regional effects of trade, migration, and productivity in China. Our paper adds to this literature by introducing demographic heterogeneity into the study of China's internal integration. This allows us to quantify how ageing changes the effects of two domestic margins, lower migration frictions and lower interregional trade costs, on aggregate welfare and spatial inequality. Our paper adds to this literature by introducing demographic heterogeneity into China's internal integration. Rather than focusing only on the direct effects of lower migration frictions and interregional trade costs, we ask how population ageing amplifies or dampens the effects of these domestic integration forces on aggregate welfare and spatial inequality.

Third, this paper relates to the literature on international trade and the Chinese economy. This literature studies how China's integration into world markets shaped exports, production, prices, productivity, and labor-market outcomes. Brandt and Lim (2024) provide a quantitative accounting of Chinese export growth and emphasize foreign demand, imported intermediates, and productivity. Caliendo, Dvorkin, and Parro (2019) quantify the dynamic regional effects of the China trade shock in a general-equilibrium framework. Our paper differs by bringing demographic change into an open-economy framework for

China. Other work highlights the role of trade policy, WTO accession, import competition, firm responses, processing trade, and productivity growth in China and abroad (Handley and Limão, 2017; Amiti et al., 2020; Autor, Dorn, and Hanson, 2013; Pierce and Schott, 2016; Yu, 2015; Brandt, Van Biesebroeck, and Zhang, 2012; Hsieh and Ossa, 2016). Our paper adds to this literature by studying demographic change in an open-economy framework for China. We focus on how ageing affects the welfare and distributional consequences of external integration.

The rest of the paper is organized as follows. Section 2 presents the stylized facts on demographic change, migration, and age-income profiles in China. Section 3 lays out the model. Section 4 describes the calibration. Section 5 presents the counterfactual results. Section 6 concludes.

2 Stylized Facts

Aggregate Demographic Trends Figure 1 plots China's annual births and deaths from 2005 to 2025, measured in units of 10,000 persons. The figure shows a sharp reversal in China's demographic dynamics. During 2005–2016, annual births remained relatively high, fluctuating around 16–18 million, while annual deaths increased only gradually from about 8.5 million to about 9.8 million. After reaching its recent peak in 2016, however, the number of births declined rapidly and persistently. By 2025, annual births had fallen to 7.92 million, less than half of the peak level observed in 2016.

A key turning point occurred in 2022, when deaths exceeded births for the first time during the sample period. Since then, the gap between the two series has continued to widen. By 2025, deaths had risen to 11.31 million, while births remained below 8 million. This divergence indicates that China has entered a phase of negative natural population growth. Although births and deaths are flow variables rather than direct measures of age composition, their reversal reflects a profound demographic transition: smaller young cohorts are entering the population, while the relative weight of older cohorts is increasing.

This aggregate pattern motivates our focus on population ageing. A declining birth rate reduces the future working-age population, while a rising number of deaths reflects the growing importance of older age groups in the population structure. These changes can affect the economy through labor supply, domestic demand, migration incentives, fiscal pressure, and regional adjustment. Therefore, population ageing is not only a demographic background condition, but also a potentially important force shaping China's spatial allocation of labor and the regional gains from domestic and external integration. The next two facts further show that this demographic transition is uneven across regions and economically relevant because workers of different ages differ in both mobility and labor income.

Regional Age Heterogeneity and Selective Migration The aggregate demographic transition documented above is not spatially uniform. Table 1 illustrates this point by comparing Guangdong, one of China's main migrant-receiving provinces, with Northeast China, a region that has experienced more advanced population ageing and net out-migration. In 2015, Guangdong had a much younger age structure: the mean age was 34.71 for the resident population and 35.00 for the hukou population. By contrast, the corresponding mean ages in Northeast China were 41.51 and 41.45. The upper tail of the age distribution shows the same contrast. Individuals aged 56 and above accounted for 25.52% of the resident population in Northeast China, compared with 16.06% in Guangdong. These differences indicate that China's population ageing is not only an aggregate trend, but also a regionally uneven process.

Table 1 further shows that internal migration is strongly age-selective. Migrants are younger than both resident and hukou populations. In Guangdong, the mean age of in-

Figure 1: China's Annual Births and Deaths

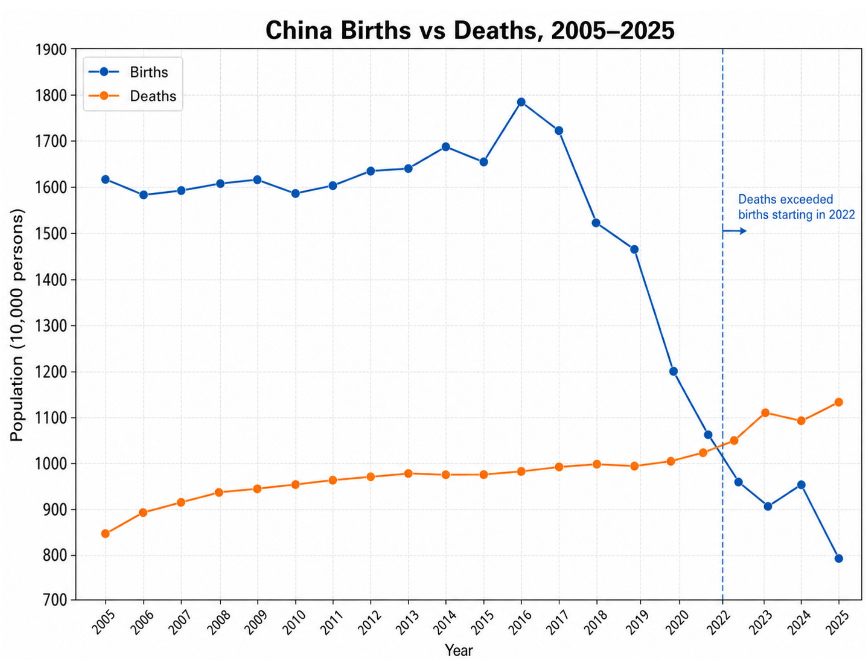

Notes: The figure plots China's total numbers of births and deaths during 2005–2025. Source: National Bureau of Statistics of China.

Table 1: Age Structure of the Population in Guangdong and Northeast China (2015)

Region	Population type	Sample size	Mean age	Ages 0–15	Ages 16–25	Ages 26–55	Ages 56–65	Ages 66+
Guangdong	Resident	158,139	34.71	17.42%	18.17%	48.35%	8.86%	7.20%
Guangdong	In-migrant	21,262	32.36	10.19%	19.98%	65.02%	3.38%	1.42%
Guangdong	Out-migrant	2,254	30.77	11.00%	23.74%	61.45%	2.44%	1.38%
Guangdong	Hukou	139,131	35.00	18.42%	17.99%	46.01%	9.59%	7.99%
Northeast	Resident	158,923	41.51	11.71%	10.57%	52.19%	15.10%	10.42%
Northeast	In-migrant	1,371	32.44	11.60%	23.49%	56.16%	5.62%	3.14%
Northeast	Out-migrant	4,777	36.86	9.17%	15.51%	58.68%	11.60%	5.05%
Northeast	Hukou	162,329	41.45	11.64%	10.60%	52.35%	15.08%	10.33%

Notes: Northeast China includes Liaoning, Jilin, and Heilongjiang. The resident population is defined by place of residence, while the Hukou population is defined by place of household registration. The in-migrant population refers to individuals whose place of residence is in the region but whose household registration is outside the region. The out-migrant population refers to individuals whose household registration is in the region but whose place of residence is outside the region. Age-group shares are calculated using unweighted individual-level observations.

migrants was 32.36, lower than the mean age of both residents and the hukou population. In Northeast China, in-migrants had a mean age of 32.44, almost nine years below the resident-population mean. Migrants were also concentrated in prime working ages: individuals aged 26–55 accounted for 65.02% of Guangdong's in-migrants and 56.16% of Northeast China's in-migrants. The scale and direction of migration flows reinforce this pattern. Guangdong received 21,262 in-migrants in the sample but sent out only 2,254 out-migrants, whereas Northeast China received 1,371 in-migrants but sent out 4,777 out-migrants. Selective migration therefore brings relatively young workers into Guangdong while removing working-age population from Northeast China.

Taken together, these patterns show that regional ageing is shaped by both local demographic structure and the age composition of migration flows. This fact is central to our model and counterfactual analysis. If workers were homogeneous, migration would only reallocate population across regions. In the data, however, migration reallocates workers with different ages, and therefore changes the regional distribution of effective labor and the strength of future migration responses. The next fact further shows why this distinction matters economically: workers of different ages do not contribute the same amount of labor income, so the age composition of regional labor supply has direct implications for real wage income and spatial inequality.

Age-Income Profile The previous two facts show that China is ageing and that age composition differs substantially across regions because migration is age-selective. These demographic patterns matter for regional economic outcomes only if workers of different ages contribute differently to effective labor supply. We therefore examine the life-cycle

Table 2: The Hump-Shape of Income and Age

	(1)	(2)	(3)	(4)	(5)	(6)
Age	0.0551***	0.0385***	0.0297***	0.0634***	0.0388***	0.0285***
	(0.0003)	(0.0002)	(0.0003)	(0.0004)	(0.0003)	(0.0003)
Age2	-0.0008***	-0.0005***	-0.0004***	-0.0009***	-0.0005***	-0.0004***
	(0.0000)	(0.0000)	(0.0000)	(0.0000)	(0.0000)	(0.0000)
Observations	1,382,263	1,382,262	1,381,554	1,345,600	1,345,600	1,344,912
Adjusted R^2	0.0596	0.6322	0.6419	0.0421	0.6305	0.6404
Implied max income age	33.4518	40.1970	37.8982	33.5509	40.0219	37.7915

Notes: This table reports regression results for how individual labor income varies with age and age squared, following Equation (1). Columns (1)–(3) use the full population sample, while Columns (4)–(6) use the working-age sample. Columns (1) and (4) include only age controls. Columns (2) and (5) additionally include gender, education, sector of employment, and region fixed effects. Columns (3) and (6) further include gender, education, marital status, ethnicity, hukou type (urban or rural), occupation, sector of employment, and region fixed effects. The implied income-maximizing age is calculated as $-\beta_1/(2\beta_2)$ in Equation (1). Standard errors are reported in parentheses. Statistical significance at the 1%, 5%, and 10% levels is indicated by ***, **, and *, respectively.

relationship between age and individual labor income. Specifically, we estimate the following quadratic specification:

$$\log(\text{Income}) = \beta_1 \times \text{Age} + \beta_2 \times \text{Age2} + \text{Controls} + \epsilon. \tag{1}$$

The dependent variable is the log of individual labor income. The control variables include gender, education, marital status, ethnicity, hukou type, occupation, sector of employment, and region fixed effects, depending on the specification.

Table 2 reports the estimation results. Across all six specifications, the coefficient on age is positive, while the coefficient on age squared is negative. Both coefficients are statistically significant at the 1% level. This pattern holds when we use the full population sample in Columns (1)–(3) and when we restrict the sample to the working-age population in Columns (4)–(6). It also remains stable after progressively adding individual characteristics and region fixed effects. The implied income-maximizing age, calculated as $-\beta_1/(2\beta_2)$, ranges from 33.45 to 40.20 across specifications. In the richer-control specifications, the peak is close to age 38.

Figure 2 provides the corresponding visual evidence. The scatter plot shows individual log labor income by age, and the fitted quadratic curve rises from young ages to prime working ages before declining at older ages. The vertical line marks the implied peak income age from the regression. The figure therefore illustrates the same life-cycle pattern as the table: labor income is not constant over age, but follows a hump-shaped profile over the life cycle.

This life-cycle income pattern gives age composition direct economic content. Since labor

Figure 2: The Hump-Shape of Income and Age

Notes: The figure plots the relationship between log labor income and age, following Equation (1). The red curve is the fitted quadratic relationship. The green vertical line indicates the implied income-maximizing age, calculated as $-\beta_1/(2\beta_2)$.

income rises over young and middle ages and declines at older ages, a region's age structure affects not only the number of workers it has, but also the amount of effective labor supplied by those workers. Combined with the previous fact that migration is age-selective, this pattern implies that internal migration can change regional effective labor supply through both the quantity and the age composition of movers.

Summary This section documents three motivating facts. First, China has entered a period of rapid demographic ageing, with births falling sharply after 2016 and deaths exceeding births since 2022. Second, ageing is spatially uneven: Guangdong remains relatively young, while Northeast China is much older, reflecting age-selective migration flows. Third, individual labor income follows a hump-shaped life-cycle profile, rising to prime working ages and declining at older ages. These facts motivate a spatial quantitative framework in which ageing affects regional effective labor supply, migration, and the gains from domestic and external integration.

3 Model

We develop a spatial trade model with multiple regions, multiple sectors, and age-specific labor mobility. The economy includes mainland Chinese province-level regions and an aggregate rest-of-world region. It has three sectors: agriculture, manufacturing, and services. Goods are traded with iceberg trade costs, and production uses labor and intermediate inputs from all sectors. Workers differ by age in labor-force participation, labor efficiency, migration frictions, and migration elasticities. Labor is mobile across Chinese regions but immobile internationally. Domestic integration operates through lower migration frictions and lower internal trade costs. The trade block follows Eaton and Kortum (2002) and Caliendo and Parro (2015), while the spatial structure builds on quantitative models of trade, migration, and regional allocation (Allen and Arkolakis, 2014; Redding and Rossi-Hansberg, 2017; Monte, Redding, and Rossi-Hansberg, 2018; Caliendo, Dvorkin, and Parro, 2019).

Ageing affects the economy through two margins. It changes regional effective labor supply because age groups differ in participation and efficiency, and it changes labor reallocation because mobility differs by age. As a result, the same changes in migration costs, internal trade costs, or external trade costs can have different aggregate and spatial effects under different age structures. The rest of this section describes the model environment, equilibrium conditions, and main mechanisms.

3.1 Preferences

Individuals are heterogeneous by age. Economic activity starts at age 16 and ends after age 65. Let

$$\mathcal{G}^W \equiv \{16, 17, \dots, 65\}$$

denote the set of working ages. For each Chinese region $n \in \mathbb{N}_0$ and age $g \in \mathcal{G}^W$, $N_{n,g}$ denotes the number of age-g individuals attached to source region n. The age distribution is exogenous. A fraction $\phi_{n,g}$ does not participate in the labor market. Each participating age-g worker supplies l^g efficiency units of labor, with $l^{16} = 1$. Before migration choices,

$$\bar{L}_{n,g} = (1 - \phi_{n,g}) N_{n,g}, \qquad \bar{L}^e_{n,g} = l^g \bar{L}_{n,g}, \tag{2}$$

where $\bar{L}_{n,g}$ is the number of participating workers and $\bar{L}^e_{n,g}$ is their effective labor endowment. Aggregating across working ages,

$$\bar{L}_n = \sum_{g \in \mathcal{G}^W} \bar{L}_{n,g}, \qquad \bar{L}^e_n = \sum_{g \in \mathcal{G}^W} \bar{L}^e_{n,g}. \tag{3}$$

A participating age-g worker in destination region n consumes sectoral composites $\{c^j_{n,g}\}_{j=1}^J$, where $c^j_{n,g}$ is consumption of sector j, and aggregate consumption $c_{n,g}$. Preferences are Cobb–Douglas across sectors and logarithmic over aggregate consumption. Let P^j_n denote the price of the sector-j composite in region n, and let P_n denote the aggregate consumption price index. Then

$$P_n = \prod_{j=1}^J \left(\frac{P^j_n}{\alpha^j_n}\right)^{\alpha^j_n}, \qquad P^j_n c^j_{n,g} = \alpha^j_n P_n c_{n,g}, \tag{4}$$

where α^j_n is the final expenditure share on sector j in region n, and $\sum_{j=1}^J \alpha^j_n = 1$. Period utility is $U(c_{n,g}) = \log(c_{n,g})$.

Following Caliendo, Dvorkin, and Parro (2019), trade imbalances are represented by regional transfers. A worker of age g in region n earns $W_n l^g$, remits a fraction φ_n of labor income, and receives a common transfer T per efficiency unit. Thus,

$$\chi_{n,g} = -\varphi_n W_n l^g + T l^g, \qquad P_n c_{n,g} = W_n l^g + \chi_{n,g}, \tag{5}$$

where

$$T = \frac{\sum_{n=1}^N \varphi_n W_n L^e_n}{\sum_{n=1}^N L^e_n}.$$

The real payoff for an age-g worker in region n is

$$\Lambda_{n,g} = \frac{W_n l^g + \chi_{n,g}}{P_n}.$$

3.2 Labor Flows

Labor is immobile internationally but mobile across Chinese regions. A participating age-g worker from source region $m \in \mathbb{N}_0$ chooses a destination region $n \in \mathbb{N}_0$, where residence and work location coincide. The indirect utility from choosing destination n is

$$V_{nm,g}(\epsilon) = \frac{z_{nm,g}(\epsilon)\Lambda_{n,g}}{\nu_{nm,g}}, \tag{6}$$

where $\nu_{nm,g}$ is the migration friction from source region m to destination region n for age group g, with $\nu_{mm,g} = 1$. The term $z_{nm,g}(\epsilon)$ is an idiosyncratic preference draw. It is i.i.d. across destinations and follows a Fréchet distribution,

$$G^g(z) = \exp\left(-z^{-\kappa^g}\right), \qquad z > 0,$$

where $\kappa^g > 0$ governs the age-specific migration response to real-payoff differences net of migration frictions.

Let $\mu_{nm,g}$ denote the share of participating age-g workers from source region m who choose destination region n. The migration shares are

$$\mu_{nm,g} = \frac{\left(\Lambda_{n,g}/\nu_{nm,g}\right)^{\kappa^g}}{\sum_{i\in\mathbb{N}_0}\left(\Lambda_{i,g}/\nu_{im,g}\right)^{\kappa^g}}, \qquad \sum_{n\in\mathbb{N}_0}\mu_{nm,g} = 1. \tag{7}$$

Destination-region labor by age is

$$L_{n,g} = \sum_{m\in\mathbb{N}_0}\mu_{nm,g}\bar{L}_{m,g}, \qquad L^e_{n,g} = l^g L_{n,g}, \tag{8}$$

where $L_{n,g}$ is the number of age-g workers in destination region n, and $L^e_{n,g}$ is their effective labor supply. Aggregating across working ages,

$$L_n = \sum_{g\in\mathcal{G}^W} L_{n,g}, \qquad L^e_n = \sum_{g\in\mathcal{G}^W} L^e_{n,g}. \tag{9}$$

For the rest of the world, L_N and L^e_N are exogenous.

Given destination labor, the regional trade imbalance associated with the transfer system is

$$D_n = \sum_{g\in\mathcal{G}^W}\chi_{n,g}L_{n,g} = -\varphi_n W_n L^e_n + T L^e_n. \tag{10}$$

3.3 Production

In each region $n = 1, \ldots, N$ and sector $j = 1, \ldots, J$, competitive firms produce a continuum of tradable varieties indexed by $\omega \in [0, 1]$. Production uses effective labor and sectoral composite intermediates:

$$y_n^j(\omega) = q_n^j(\omega)\big(\ell_n^j(\omega)\big)^{\gamma_n^j} \prod_{k=1}^{J} \big(m_n^{jk}(\omega)\big)^{\gamma_n^{jk}}, \tag{11}$$

where $y_n^j(\omega)$ is output, $q_n^j(\omega)$ is variety productivity, $\ell_n^j(\omega)$ is effective labor, and $m_n^{jk}(\omega)$ is the sector-k composite input used in sector-j production. The parameter γ_n^j is the value-added share, and γ_n^{jk} is the share of sector-k intermediates in sector-j production. Constant returns imply

$$\gamma_n^j + \sum_{k=1}^{J} \gamma_n^{jk} = 1.$$

Productivity follows Eaton and Kortum (2002). For each region-sector pair, $q_n^j(\omega)$ is drawn from

$$F_n^j(q) = \exp\big(-\lambda_n^j q^{-\theta}\big),$$

where λ_n^j is the productivity parameter and $\theta > 0$ governs dispersion. Cost minimization gives the unit cost of producing a sector-j variety in region n:

$$c_n^j = \Upsilon_n^j W_n^{\gamma_n^j} \prod_{k=1}^{J} (P_n^k)^{\gamma_n^{jk}}, \qquad \Upsilon_n^j = (\gamma_n^j)^{-\gamma_n^j} \prod_{k=1}^{J} (\gamma_n^{jk})^{-\gamma_n^{jk}}. \tag{12}$$

Here, c_n^j is the unit cost net of the variety-specific productivity draw.

3.4 Trade

Goods are traded across Chinese regions and with the rest of the world subject to iceberg costs. Shipping one unit of a sector-j variety from region i to region n requires $\kappa_{ni}^j \geq 1$ units, with $\kappa_{nn}^j = 1$.

In each region n, sector-j varieties are aggregated into a CES composite Q_n^j with elasticity $\sigma^j > 1$. Standard Eaton–Kortum arguments imply

$$P_n^j = A^j \left[\sum_{i=1}^{N} \lambda_i^j (\kappa_{ni}^j c_i^j)^{-\theta}\right]^{-1/\theta}, \qquad A^j = \left[\Gamma\left(\frac{1+\theta-\sigma^j}{\theta}\right)\right]^{\frac{1}{1-\sigma^j}}. \tag{13}$$

The share of region n's expenditure on sector-j goods sourced from region i is

$$\pi^j_{ni} = \frac{\lambda^j_i (c^j_i \kappa^j_{ni})^{-\theta}}{\sum_{m=1}^N \lambda^j_m (c^j_m \kappa^j_{nm})^{-\theta}}. \tag{14}$$

3.5 Aggregation and Market Clearing

Aggregate final consumption in region n is $C_n = \sum_{g \in \mathcal{G}^W} c_{n,g} L_{n,g}$, with sectoral consumption $C^j_n = \sum_{g \in \mathcal{G}^W} c^j_{n,g} L_{n,g}$. Since workers in the same region face the same Cobb–Douglas expenditure shares, $P^j_n C^j_n = \alpha^j_n P_n C_n$. Aggregating worker budget constraints gives

$$P_n C_n = W_n L^e_n + D_n, \qquad D_n = -\varphi_n W_n L^e_n + T L^e_n, \qquad \sum_{n=1}^N D_n = 0.$$

Let $X^j_n \equiv P^j_n Q^j_n$ denote total expenditure in region n on the sector-j composite, and let Y^j_n denote sales of sector j produced in region n. Total sectoral expenditure equals final plus intermediate demand,

$$X^j_n = \alpha^j_n P_n C_n + \sum_{k=1}^J \gamma^{kj}_n Y^k_n,$$

where γ^{kj}_n is the share of sector-k sales spent on sector-j intermediate inputs. Goods- and labor-market clearing require

$$Y^j_n = \sum_{i=1}^N \pi^j_{in} X^j_i, \qquad W_n L^e_n = \sum_{j=1}^J \gamma^j_n Y^j_n.$$

These conditions determine regional expenditure, sales, trade imbalances, and labor payments given prices, trade shares, and effective labor.

Equilibrium Definition The model is characterized by demographic objects $\{N_{n,g}, \phi_{n,g}, l^g\}$, preference parameters $\{\alpha^j_n\}$, technology parameters $\{\lambda^j_n, \gamma^j_n, \gamma^{jk}_n, \theta, \sigma^j\}$, bilateral trade costs $\{\kappa^j_{ni}\}$, migration frictions $\{\nu_{nm,g}\}$, migration elasticities $\{\kappa^g\}$, and transfer wedges $\{\varphi_n\}$. Chinese regions are indexed by $n \in \mathbb{N}_0$, and region N denotes the rest of the world.

Given these objects, a competitive equilibrium consists of wages, prices, migration shares, labor allocations, production, expenditure, trade flows, and transfers such that workers choose destinations given real payoffs and migration frictions; firms minimize costs under constant-returns technologies, Fréchet productivity draws, and iceberg trade costs; final and intermediate demands are consistent with household and firm optimization; and goods and labor markets clear, with aggregate transfers balanced across regions. Appendix Table A.1 lists the full set of equilibrium conditions.

4 Calibration

This section describes the calibration of the benchmark economy. The model includes 30 mainland Chinese province-level regions, excluding Tibet, and one aggregated rest-of-world region, so $N = 31$. Chinese regions are indexed by $n \in \mathbb{N}_0 = 1, \ldots, 30$, while region N denotes the rest of the world. The model has three sectors—agriculture, manufacturing, and services—and three working-age groups: young, middle, and old.

The calibration uses four main data sources. The 2005 National 1% Population Sample Survey is used to estimate the age-efficiency profile l^g and age-specific migration elasticities κ^g, because it reports age, individual income, and labor-market characteristics (National Bureau of Statistics of China, 2007). The 2015 National 1% Population Sample Survey is used to construct population shares by age and source region, labor-force participation rates, and age-specific migration shares (Department of Population and Employment Statistics, National Bureau of Statistics of China, 2016). Source region is measured by hukou registration or hukou ID-number location, and destination region by current residence or work location. Chinese provincial MRIO tables are used to construct internal trade flows, production shares, input-output shares, final expenditure shares, and regional trade imbalances (Zheng et al., 2021; Zhao et al., 2024). OECD ICIO tables provide China–rest-of-world trade flows and production and expenditure objects for the rest of the world (Yamano et al., 2021; OECD, 2021). Penn World Table data provide aggregate population and labor input for China and the rest of the world (Feenstra, Inklaar, and Timmer, 2015; Groningen Growth and Development Centre, 2021). All value variables are in millions of U.S. dollars, and the Chinese MRIO table is rescaled to match China's aggregate value added in the OECD ICIO table.

The calibration proceeds in three steps, which structure the subsections that follow. First, we assign time-invariant parameters, including elasticities and age-specific labor and migration parameters. Second, we construct the objects directly observed from the demographic, trade, and input-output data. Third, we recover the remaining fundamentals from the model's equilibrium conditions, including productivity, bilateral trade costs, and migration frictions. The following subsections provide the details for each calibrated object.

4.1 Exogenous Parameters

Age-Efficiency Profile The age-efficiency profile l^g captures the number of efficiency units supplied by one participating age-g worker. We estimate this profile from the 2005 National 1% Population Sample Survey, the only available micro-level population dataset that jointly reports age, individual income, and labor-market characteristics (National Bureau of Statistics of China, 2007). Specifically, we regress log individual labor income on age dummies and a set of individual controls:

$$\log y_i = \sum_{g \in \mathcal{G}^W} \beta_g \mathbf{1}\{age_i = g\} + X_i' \Gamma + \varepsilon_i, \tag{15}$$

where i indexes individuals, y_i is individual labor income, and X_i includes controls such as gender, education, marital status, ethnicity, hukou type (urban or rural), occupation, sector of employment, and region fixed effects. The age fixed effects capture the life-cycle component of labor efficiency after controlling for observable individual characteristics. We normalize labor efficiency for the youngest working age group to one and construct

$$l^g = \exp(\beta_g - \beta_{16}). \tag{16}$$

Table 3: Age Group Efficiency

	(1)	(2)	(3)	(4)	(5)	(6)
$\mathbf{1}\{age_i = [26, 55]\}$	0.0513***	0.1474***	0.0623***			
	(0.0021)	(0.0014)	(0.0018)			
$\mathbf{1}\{age_i = [56, 65]\}$	-0.4915***	0.0002	-0.0888***			
	(0.0033)	(0.0022)	(0.0026)			
$\mathbf{1}\{age_i = [30, 51]\}$				-0.0020	0.1114***	0.0367***
				(0.0018)	(0.0012)	(0.0014)
$\mathbf{1}\{age_i = [52, 65]\}$				-0.4389***	0.0067***	-0.0729***
				(0.0025)	(0.0017)	(0.0019)
Observations	1,345,600	1,345,600	1,344,912	1,345,600	1,345,600	1,344,912
Adjusted R^2	0.0259	0.6290	0.6393	0.0291	0.6276	0.6388

Notes: The table reports age-related labor efficiency, relative to the youngest working age group, with individual labor income as dependent variable. Columns (1)–(3) use age groups 16–25, 26–55, and 56–65; while Columns (4)–(6) use age groups 16–29, 30–51, and 52–65, respectively. Columns (1) and (4) only consider age group indicators, Columns (2) and (5) include gender, education, sector of employment, and region fixed effects; Columns (3) and (6) includes gender, education, marital status, ethnicity, hukou type (urban or rural), occupation, sector of employment, and region fixed effects. Standard errors are presented in parentheses. Statistical significance at the 1%, 5%, and 10% levels is indicated by ***, **, and *, respectively.

Table 3 reports the labor efficiency for different age groups. It can be seen clearly that the middle age group has the highest labor efficiency, compared to the youngest or oldest group. The estimates are robust to different age group classifications and with detailed individual characteristics controlled for. In the following content, we choose the estimates of column (3) as the benchmark, as more individual control variables are incorporated and the age grouping seems more reasonable. Thus, the age-efficiency profiles l^g for young, middle, and old groups are 1.00, 1.06, and 0.92, respectively.[1]

Age-Related Migration Elasticities To estimate age-related migration elasticities κ^a for each of the three age groups using census-based migration flows, we can follow the income-dispersion method in Tombe and Zhu (2019). Under the Fréchet migration structure, log real earnings follow a Gumbel distribution with standard deviation $\pi/(\kappa\sqrt{6})$, so the migration elasticity can be inferred from within-group dispersion in log earnings. In practice, for each age group a, we compute the within-group standard deviation of log nominal earnings in the 2005 Population Survey, where groups are defined by source region, destination region, sector of employment, and age group, and then recover

$$\kappa^a = \frac{\pi}{\sqrt{6}\, sd_a(\log y)}.$$

It turns out that age-specific migration elasticities are 3.21, 2.68, 2.21 for young, middle, and old labor groups, respectively. A larger elasticity implies a worker is more sensitive to the migration costs and thus has more willingness to mobilize given the same migration cost shocks. Clearly, the estimates indicate that younger workers are more likely to migrate relative to the older within China.

Other Time-Invariant Elasticities We set the trade elasticity to $\theta = 4$ in the benchmark calibration, following Simonovska and Waugh (2014). The within-sector elasticity of substitution across varieties is set to $\sigma^j = 2$ for all three sectors, following the estimates and calibration practice in Broda and Weinstein (2006).

Population, Labor Force, and Effective Labor We construct population and labor-force objects from the 2015 population survey and aggregate population data (Department of Population and Employment Statistics, National Bureau of Statistics of China, 2016).

[1] Given the estimates of column (3) in Table 3, we have $\exp(0.0623) \approx 1.06$ for middle age group and $\exp(-0.0888) \approx 0.92$ for old age group, with young age group efficiency normalized to 1.

The number of age-g individuals attached to source region n, $N_{n,g}$, is identified by hukou registration or hukou ID-number location. Labor-force participation $\tau_{n,g}$ is measured by age and destination region, where destination is identified by current residence or work location; non-participation is $\phi_{n,g} = 1 - \tau_{n,g}$.

Using census sampling weights, we compute age distributions by source region and combine them with aggregate population totals. Participating workers before migration are $\bar{L}_{n,g} = \tau_{n,g} N_{n,g}$. After migration choices, destination-region labor is $L_{n,g} = \sum_{m \in \mathbb{N}_0} \mu_{nm,g} \bar{L}_{m,g}$, and effective labor is $L_n^e = \sum_{g \in \mathcal{G}^W} l^g L_{n,g}$. For the rest of the world, labor is internationally immobile, so L_N^e is taken from Penn World Table aggregate labor data (Feenstra, Inklaar, and Timmer, 2015; Groningen Growth and Development Centre, 2021).

Production Shares and Input–Output Linkages We calibrate production shares from input–output data (Zhao et al., 2024). Let GO_n^j and VA_n^j denote gross output and value added in sector j and region n, and let M_n^{jk} denote sector-k intermediate inputs used in sector-j production. We set

$$\gamma_n^j = \frac{VA_n^j}{GO_n^j}, \qquad \gamma_n^{jk} = \frac{M_n^{jk}}{GO_n^j}, \qquad \gamma_n^j + \sum_{k=1}^{J} \gamma_n^{jk} = 1. \tag{17}$$

Thus, γ_n^j is the value-added share, and γ_n^{jk} is the share of sector-k intermediate inputs in sector-j production.

Final Expenditure Shares and Trade Imbalances Let FD_n^j denote final expenditure on sector j in region n, and let X_{ni}^j denote region n's expenditure on sector-j goods from region i. We set $\alpha_n^j = FD_n^j / \sum_{k=1}^J FD_n^k$, $X_n^j = FD_n^j + \sum_{k=1}^J M_n^{kj}$, and $\pi_{ni}^j = X_{ni}^j / X_n^j$, with $\sum_{j=1}^J \alpha_n^j = 1$. Here, X_n^j includes both final and intermediate demand for sector-j goods.

Regional trade imbalance is total expenditure minus total sales, $D_n^{data} = \sum_{j=1}^J X_n^j - \sum_{j=1}^J Y_n^j$, where Y_n^j is total sales of sector j produced in region n. A positive D_n^{data} denotes a trade deficit. The transfer wedge φ_n matches this imbalance through $D_n^{data} = -\varphi_n W_n L_n^e + TL_n^e$, where $T = \sum_{n=1}^N \varphi_n W_n L_n^e / \sum_{n=1}^N L_n^e$. Since only net transfers matter, we normalize $T = 0$, implying $\varphi_n = -D_n^{data}/(W_n L_n^e)$.

4.2 Exogenous Shocks

This subsection calibrates productivity parameters, bilateral trade costs, and migration frictions.

Fundamental Productivity We calibrate the sector- and region-specific productivity parameter λ_n^j from the Eaton–Kortum price index and the home expenditure share:

$$\lambda_n^j = \pi_{nn}^j \left(\frac{A^j c_n^j}{P_n^j} \right)^{\theta}, \qquad A^j = \left[\Gamma \left(\frac{1+\theta-\sigma^j}{\theta} \right) \right]^{\frac{1}{1-\sigma^j}}. \tag{18}$$

Here, c_n^j is the unit cost of producing sector j in region n. Labor-market clearing gives $W_n = \sum_{j=1}^J \gamma_n^j Y_n^j / L_n^e$. Given wages, input shares, and sectoral prices,

$$c_n^j = \Upsilon_n^j W_n^{\gamma_n^j} \prod_{k=1}^J (P_n^k)^{\gamma_n^{jk}}, \qquad \Upsilon_n^j = (\gamma_n^j)^{-\gamma_n^j} \prod_{k=1}^J (\gamma_n^{jk})^{-\gamma_n^{jk}}.$$

I construct sectoral prices P_n^j following Sposi, Yi, and Zhang (2025). Specifically, We use the production structure and sectoral value-added prices reported in the China Statistical Yearbook to back out sectoral gross-output prices P_n^j. Appendix B.2 provides the details. Given W_n, P_n^j, and the input-output cost shares, We compute c_n^j. We then use the observed home share π_{nn}^j and equation (18) to recover the productivity parameter λ_n^j. The fundamental productivity reported in the quantitative analysis is $(\lambda_n^j)^{1/\theta}$.

Bilateral Trade Costs After recovering λ_n^j and c_n^j, we back out bilateral trade costs from the sectoral trade-share equation. Taking the ratio of bilateral expenditure to home expenditure gives

$$\kappa_{ni}^j = \left[\left(\frac{\pi_{ni}^j}{\pi_{nn}^j} \right) \frac{\lambda_n^j (c_n^j)^{-\theta}}{\lambda_i^j (c_i^j)^{-\theta}} \right]^{-1/\theta}, \qquad \kappa_{nn}^j = 1. \tag{19}$$

Here, π_{ni}^j is region n's expenditure share on sector-j goods sourced from region i, computed from the input-output tables.

Migration Shares and Migration Frictions We construct age-specific migration shares from census micro data. Let $M_{nm,g}$ denote the number of age-g individuals with source region m and destination region n, where source is identified by hukou location and destination by current residence or work location. Migration shares are

$$\mu_{nm,g} = \frac{M_{nm,g}}{\sum_{i \in \mathbb{N}_0} M_{im,g}}, \qquad \sum_{n \in \mathbb{N}_0} \mu_{nm,g} = 1.$$

Using the migration-choice equation, the stayer normalization $\nu_{mm,g} = 1$, and the stayer share as reference, we recover

$$\nu_{nm,g} = \left(\frac{\mu_{nm,g}}{\mu_{mm,g}}\right)^{-1/\kappa^g} \frac{\Lambda_{n,g}}{\Lambda_{m,g}}, \qquad n \neq m, \tag{20}$$

where the real payoff is $\Lambda_{n,g} = (W_n l^g + \chi_{n,g})/P_n$. Thus, conditional on real-payoff differences, lower migration shares imply higher migration frictions.

4.3 Calibration Results and Model Fit

This subsection summarizes the calibration results and evaluates the calibration by feeding the calibrated parameters and wedges back into the model. We compare model-generated wages, sectoral expenditures, trade shares, and migration shares with their data counterparts.

Table 4 reports the main calibrated parameters and exogenous objects in the benchmark economy. For objects varying across regions, sectors, ages, or bilateral pairs, the table reports the mean and the 25th, 50th, and 75th percentiles in parentheses. Sector-specific objects are reported for agriculture, manufacturing, and services, denoted by a, m, and s. For γ_n^{jk}, moments are reported by producing sector j, pooling over regions and input sectors. Fundamental productivity, trade costs, and migration frictions report weighted means using value added, bilateral trade flows, and bilateral migration flows, respectively; percentile moments are unweighted. Fundamental productivity is normalized relative to Beijing. Trade costs and migration frictions exclude own-region observations.

Table 4: Calibration Summary

Object	**Notation**	**Value / Moments**	**Source / Method**
Panel A. Parameters			
Trade elasticity	θ	4	Following Simonovska and Waugh (2014)
Variety elasticity	σ^j	2, $\forall j$	Following Broda and Weinstein (2006)
Migration elasticity	κ^g	{3.21, 2.68, 2.21}	2005 Population Survey
Age-efficiency profile	l^g	{1.00, 1.06, 0.92}	2005 Population Survey
Labor shares	γ_n^a	0.59 (0.57, 0.59, 0.65)	China MRIO and OECD ICIO tables
	γ_n^m	0.26 (0.22, 0.24, 0.29)	China MRIO and OECD ICIO tables
	γ_n^s	0.46 (0.44, 0.46, 0.47)	China MRIO and OECD ICIO tables
Input-output shares	γ_n^{ak}, $\forall k$	0.19 (0.05, 0.16, 0.26)	China MRIO and OECD ICIO tables
	γ_n^{mk}, $\forall k$	0.19 (0.06, 0.14, 0.25)	China MRIO and OECD ICIO tables
	γ_n^{sk}, $\forall k$	0.18 (0.07, 0.14, 0.26)	China MRIO and OECD ICIO tables
Final expenditure shares	α_n^a	0.05 (0.03, 0.05, 0.06)	China MRIO and OECD ICIO tables

Continued on next page

Table 4: Calibration Summary (continued)

Object	Notation	Value / Moments	Source / Method
	α_n^m	0.24 (0.21, 0.25, 0.27)	China MRIO and OECD ICIO tables
	α_n^s	0.71 (0.68, 0.71, 0.76)	China MRIO and OECD ICIO tables
Panel B. Exogenous shocks			
Fundamental productivity	$(\lambda_n^a)^{1/\theta}$	0.40 (0.16, 0.25, 0.28)	Home shares, prices, and unit costs
	$(\lambda_n^m)^{1/\theta}$	0.68 (0.57, 0.79, 1.04)	Home shares, prices, and unit costs
	$(\lambda_n^s)^{1/\theta}$	0.23 (0.34, 0.39, 0.42)	Home shares, prices, and unit costs
Migration frictions	ν_{nm,g_1}	8.16 (5.81, 9.28, 16.75)	Migration shares and real payoffs
	ν_{nm,g_2}	11.73 (10.71, 17.71, 31.13)	Migration shares and real payoffs
	ν_{nm,g_3}	28.53 (30.69, 73.16, 100.00)	Migration shares and real payoffs
Migration frictions, all age groups	$\nu_{nm,g}, \forall g$	11.75 (9.40, 20.15, 65.93)	Migration shares and real payoffs
Internal trade costs	κ_{ni}^a	1.75 (4.02, 13.03, 40.04)	Price and trade-share inversion
	κ_{ni}^m	2.07 (2.01, 2.71, 3.81)	Price and trade-share inversion
	κ_{ni}^s	2.58 (2.60, 3.60, 5.86)	Price and trade-share inversion
Internal trade costs, all sectors	$\kappa_{ni}^j,\ \forall j$	2.23 (2.44, 3.75, 8.20)	Price and trade-share inversion
External trade costs	κ_{ni}^a	3.02 (2.46, 4.28, 11.60)	Price and trade-share inversion
	κ_{ni}^m	2.96 (1.76, 3.37, 6.29)	Price and trade-share inversion
	κ_{ni}^s	3.97 (4.89, 10.15, 22.56)	Price and trade-share inversion
External trade costs, all sectors	$\kappa_{ni}^j,\ \forall j$	3.13 (2.40, 5.63, 10.83)	Price and trade-share inversion
Population shares	s_{n,g_1}^N	0.24 (0.12, 0.16, 0.18)	Population Survey and macro totals
	s_{n,g_2}^N	0.63 (0.66, 0.67, 0.69)	Population Survey and macro totals
	s_{n,g_3}^N	0.14 (0.14, 0.17, 0.20)	Population Survey and macro totals
Participation rate	τ_{n,g_1}	0.46 (0.42, 0.47, 0.50)	Population Survey
	τ_{n,g_2}	0.76 (0.73, 0.76, 0.79)	Population Survey
	τ_{n,g_3}	0.43 (0.39, 0.46, 0.48)	Population Survey
Trade imbalance wedges	φ_n	−0.09 (−0.14, −0.00, 0.06)	Matched to regional trade deficits

Notes: This table reports the main parameters and calibrated objects in the benchmark economy. For varying objects, entries report the mean and the 25th, 50th, and 75th percentiles in parentheses, except for population shares. For population shares, the first number is the national age-group share, $s_g^N = \sum_n N_{n,g} / \sum_n \sum_{g'} N_{n,g'}$, while parentheses report percentiles of regional age-group shares, $s_{n,g}^N = N_{n,g} / \sum_{g'} N_{n,g'}$. Sectors a, m, and s denote agriculture, manufacturing, and services. For γ_n^{jk}, moments pool over regions and input sectors within each producing sector j. Means for productivity, trade costs, and migration frictions are weighted by value added, trade flows, and migration flows, respectively; percentiles are unweighted. Fundamental productivity is normalized to Beijing. Trade-cost and migration-friction moments exclude own-region observations. Trade elasticity, variety elasticity, migration elasticity, and the age-efficiency profile use the 2005 calibration; other moments use 2017 data, except migration shares, which use 2015 data to approximate 2017 migration patterns.

Panel A summarizes the time-invariant parameters and calibrated production and expenditure shares. The migration elasticity declines with age, from 3.21 for young workers to 2.21 for old workers, implying that younger workers are more responsive to real-payoff differences. The age-efficiency profile is hump-shaped, with middle-age workers supplying the most efficiency units. Across sectors, the labor share is highest in agriculture and lowest in manufacturing, while manufacturing is more intensive in intermediate inputs. Final expenditure is concentrated in services, followed by manufacturing and agriculture.

Panel B reports the recovered shocks and wedges. Fundamental productivity is normalized relative to Beijing and varies substantially across sectors and regions. Manufacturing has the highest typical productivity and the largest interquartile dispersion, while services are more tightly clustered in the unweighted regional distribution. Migration frictions rise sharply with age: the weighted mean increases from 8.16 for young workers to 28.53 for old workers, consistent with lower mobility among older workers. For internal trade costs, the weighted mean is highest in services and lowest in agriculture, but agriculture has very large unweighted percentiles, indicating that many agricultural region pairs have high trade costs but receive little trade-flow weight. External trade costs are also highest in services and lowest in manufacturing. Population shares show that the middle-age group is the largest working-age group, participation rates peak for middle-age workers, and the trade-imbalance wedge is centered near zero but varies across regions.

Figure 3 reports the model fit. The four panels compare data on the x-axis with model-generated values on the y-axis for log wages, log sectoral expenditures, trade shares, and migration shares. The points lie close to the 45-degree line, showing that the calibrated model reproduces the main patterns in the data.

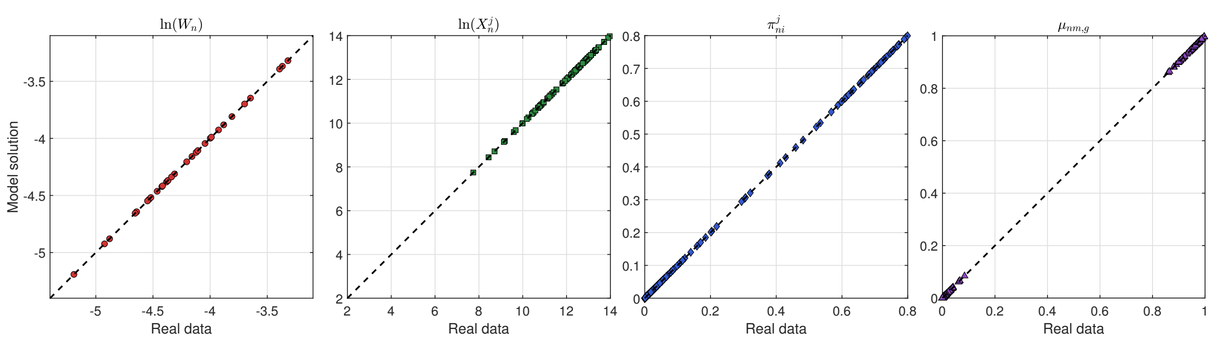

Figure 3: Model Fit

Notes: The scatter plots display data on the x-axis and model-generated values on the y-axis. The four panels report log wages, log sectoral expenditures, trade shares, and migration shares. The dashed line denotes the 45-degree reference line.

Overall, the calibration matches the main data patterns well. We next use the calibrated model to quantify the economic importance of the underlying forces.

5 Quantitative Analysis

This section quantifies the effects of population ageing, domestic integration, and external integration on welfare and spatial inequality. We use the calibrated 2017 economy as the benchmark and construct counterfactuals by resetting selected fundamentals to their 1997 values. Relative to 1997, the 2017 economy has an older labor-force age distribution, lower domestic migration costs, lower internal trade costs, and lower China–ROW trade costs. The counterfactuals mute selected 2017 forces while holding all other fundamentals at their benchmark values. Subsection 5.1 describes the design; Subsections 5.2 and 5.3 report aggregate and provincial effects.

5.1 Counterfactual Design

We construct the counterfactuals from the calibrated 1997 and 2017 economies, using the same model structure and calibration procedure. The 2017 economy is the benchmark, while the 1997 economy provides the values used to mute selected 2017 forces. For migration objects, the 1997 calibration uses the 2000 population census micro data, while the 2017 benchmark uses the 2015 National 1% Population Sample Survey.

We use hat notation to summarize these changes. For any block of fundamentals z, the calibrated 1997 value relative to its 2017 benchmark value is

$$\widehat{z} \equiv \frac{z_{1997}}{z_{2017}}. \tag{21}$$

Applying this shock to the 2017 benchmark resets the corresponding block to its 1997 calibrated value. The relevant blocks are the population age distribution, domestic migration costs, internal trade costs, and China–ROW trade costs. The demographic shock is applied to population shares, holding aggregate population fixed at its 2017 level, while friction shocks are applied element by element to the corresponding bilateral objects.

Table 5 summarizes these four shock blocks. The reported moments are descriptive; the counterfactuals use the full vectors or matrices of calibrated shocks. The table shows that, from 1997 to 2017, the labor-force age distribution became older, domestic migration costs fell, internal trade costs fell, and China–ROW trade costs fell. The young-age share ratio is 1.21, while the old-age share ratio is 0.79. Migration frictions, internal trade costs, and external trade costs are all higher in 1997, with pooled weighted mean ratios of 1.95, 1.26, and 1.42, respectively.

Table 5: Moments Used to Construct Counterfactual Shocks

Object	Notation	Mean Ratio	p25, p50, p75 Ratios
Panel A. Demographic ageing: 1997 relative to 2017			
Change in population shares	$\widehat{s}^N_{g_1}$	1.21	(1.75, 1.44, 1.50)
	$\widehat{s}^N_{g_2}$	0.97	(0.97, 1.00, 0.99)
	$\widehat{s}^N_{g_3}$	0.79	(0.64, 0.59, 0.55)
Panel B. Domestic integration: migration frictions, 1997 relative to 2017			
Change in migration frictions	$\widehat{\nu}_{nm,g_1}$	2.15	(1.56, 2.02, 5.97)
	$\widehat{\nu}_{nm,g_2}$	1.86	(1.40, 1.59, 3.21)
	$\widehat{\nu}_{nm,g_3}$	2.17	(2.86, 1.37, 1.00)
	$\widehat{\nu}_{nm,g},\ \forall g$	1.95	(1.62, 2.99, 1.52)
Panel C. Domestic integration: internal trade costs, 1997 relative to 2017			
Change in internal trade costs	$\widehat{\kappa}^a_{ni}$	1.69	(0.77, 0.28, 0.12)
	$\widehat{\kappa}^m_{ni}$	1.27	(1.29, 1.12, 0.93)
	$\widehat{\kappa}^s_{ni}$	1.34	(1.34, 1.16, 0.85)
	$\widehat{\kappa}^j_{ni},\ \forall j$	1.26	(1.21, 0.95, 0.55)
Panel D. External integration: China–ROW trade costs, 1997 relative to 2017			
Change in external trade costs	$\widehat{\kappa}^a_{nN}, \widehat{\kappa}^a_{Nn}$	1.93	(1.26, 1.43, 1.13)
	$\widehat{\kappa}^m_{nN}, \widehat{\kappa}^m_{Nn}$	1.31	(1.24, 0.96, 1.68)
	$\widehat{\kappa}^s_{nN}, \widehat{\kappa}^s_{Nn}$	2.08	(1.02, 0.84, 0.55)
	$\widehat{\kappa}^j_{nN}, \widehat{\kappa}^j_{Nn},\ \forall j$	1.42	(1.20, 1.18, 1.10)

Notes: All entries are 1997 values relative to 2017 values. Panel A reports changes in population shares, not levels. The first number is the ratio of the national age-group share, $s^N_g = \sum_n N_{n,g} / \sum_n \sum_{g'} N_{n,g'}$; parentheses report ratios of the 25th, 50th, and 75th percentiles of regional age-group shares, $s^N_{n,g} = N_{n,g} / \sum_{g'} N_{n,g'}$. For migration frictions, internal trade costs, and external trade costs, the first number is the ratio of weighted means, with parentheses reporting percentile ratios. Weights are migration flows, internal trade flows, and external trade flows, respectively. Domestic trade costs and migration frictions exclude own-region observations; external trade costs include only China–ROW and ROW–China observations.

Using these shock blocks, the counterfactuals mute selected 2017 forces one at a time and in combination. The next subsections report the resulting aggregate effects, spatial inequality, and provincial reallocation, with all outcomes normalized by the 2017 benchmark.

5.2 Aggregate Effects and Spatial Inequality

This subsection reports aggregate real wage and cross-province dispersion. The main aggregate statistic is RW_{pew}, real wage income per effective worker. The distributional statistic is $Gini_{RW,pew}$, the Gini coefficient of W_n/P_n across Chinese regions. All entries are normalized by the 2017 benchmark, Case 0.

Domestic and External Frictions Table 6 starts from the fact that the 1997–2017 change combines an older age structure with lower domestic and external frictions. The first comparison isolates the age structure. When the age distribution is reset to its 1997 value, holding aggregate population fixed, RW_{pew} rises from 1.0000 to 1.0046, while $Gini_{RW,pew}$ falls from normalized 1.0000 to 0.9913. Thus, moving from the younger 1997 age structure to the older 2017 level lowers aggregate real wage income per effective worker by 0.46 percent and raises spatial dispersion in real wages by 0.87 percent. This experiment changes the composition of the population, not its aggregate size. The mechanism works through age-specific labor efficiency and mobility. Younger workers have stronger migration responses and face different migration frictions, so a younger age structure reallocates effective labor more readily toward high-return regions. Ageing weakens this reallocation margin.

Table 6: Counterfactual Results: Domestic and External Frictions

	Case 0	**Case 1A**	**Case 2A**	**Case 1B**	**Case 2B**
Set to 1997	None	Dom. MC	Dom. TC	Dom. MCTC	Ext. TC
RW_{pew}	1.0000	0.9756	0.9218	0.9057	0.9687
$Gini_{RW,pew}$	1.0000	1.0447	1.0155	1.0379	0.9585
	Case X	**Case 1AX**	**Case 2AX**	**Case 1BX**	**Case 2BX**
Set to 1997	Age dist.	Age dist. & Dom. MC	Age dist. & Dom. TC	Age dist. & Dom. MCTC	Age dist. & Ext. TC
RW_{pew}	1.0046	0.9815	0.9250	0.9097	0.9729
$Gini_{RW,pew}$	0.9913	1.0300	1.0093	1.0299	0.9504

Notes: All entries are normalized by Case 0. Each counterfactual sets the listed fundamentals to their 1997 calibrated values and keeps all other fundamentals at the 2017 benchmark. The upper block keeps the 2017 age distribution and changes only the listed friction blocks to their 1997 values. The lower block repeats the same exercises but also sets the age distribution to its 1997 value. "Age dist." denotes the population age distribution. "Dom. MC" denotes domestic migration costs, "Dom. TC" denotes domestic trade costs, "Dom. MCTC" denotes domestic migration costs and domestic trade costs jointly, and "Ext. TC" denotes external trade costs. $RW_{pew} = \sum_n W_n L_n^e / P_n / \sum_n L_n^e$ is aggregate real wage income per effective worker. $Gini_{RW,pew}$ is the Gini coefficient of W_n/P_n across Chinese regions.

To measure how ageing changes the effect of each integration force, we compare the same force under the 2017 and 1997 age structures. For an integration force f, the effect under the 2017 age structure is

$$E_f^{2017} = (1 - \text{Case } f) \times 100\%.$$

Under the 1997 age structure, the effect is computed relative to Case X:

$$E_f^{1997} = \frac{\text{Case X} - \text{Case } fX}{\text{Case X}} \times 100\%.$$

The relative effect of ageing is

$$\frac{E_f^{2017} - E_f^{1997}}{E_f^{1997}} \times 100\%.$$

For RW_{pew}, a positive value of E_f means that the 2017 integration force raises aggregate real wages. For $Gini_{RW,pew}$, a positive value means that the force raises spatial dispersion, while a negative value means that it reduces spatial dispersion.

The upper block of Table 6 isolates the market-integration margins under the 2017 age structure. Domestic migration integration raises RW_{pew} by $(1 - 0.9756) \times 100\% = 2.44$ percent. Domestic trade integration raises RW_{pew} by $(1 - 0.9218) \times 100\% = 7.82$ percent, and the joint domestic package raises it by $(1 - 0.9057) \times 100\% = 9.43$ percent. External integration raises RW_{pew} by $(1 - 0.9687) \times 100\% = 3.13$ percent. Hence, the largest direct real-wage effect comes from domestic trade integration. The reason is that lower domestic trade costs improve goods-market access and reduce the cost of intermediate inputs across provinces, so the gain operates through the production and goods-flow margin. Lower migration costs also raise aggregate real wages, but their primary role is to move workers across space rather than to lower the cost of goods and intermediate inputs.

The lower block of Table 6 shows how these real-wage effects change under the younger 1997 age structure. For domestic migration integration, the real-wage gain is $E_{\text{MC}}^{2017} = 2.44\%$ under the 2017 age structure and $E_{\text{MC}}^{1997} = 2.30\%$ under the 1997 age structure. Thus, ageing raises the real-wage effect of domestic migration integration by 6.1%. In an older economy, migration frictions become more binding for aggregate real wages. A less mobile labor force leaves more effective labor attached to regions where real payoffs are relatively low. Lowering migration frictions then relaxes this constraint and reallocates effective labor toward higher-return regions. Even if the migration response is weaker in quantity terms, the marginal real-wage value of reducing migration frictions can be larger because the initial allocation is more constrained.

For domestic trade integration, the real-wage gain is $E_{\text{TC}}^{2017} = 7.82\%$, compared with $E_{\text{TC}}^{1997} = 7.92\%$, so ageing reduces the effect by 1.3%. For the joint domestic package, the gain is $E_{\text{MCTC}}^{2017} = 9.43\%$, compared with $E_{\text{MCTC}}^{1997} = 9.45\%$, so ageing reduces the effect by 0.2%. For external integration, the gain is $E_{\text{Ext}}^{2017} = 3.13\%$, compared with $E_{\text{Ext}}^{1997} = 3.16\%$, so ageing reduces the effect by about 0.8%. Hence, ageing amplifies the gain from lowering migration frictions but slightly dampens the real-wage gains from lower domestic trade costs and lower China–ROW trade costs.

Combined Domestic and External Frictions Table 7 combines domestic and external integration using the same comparison as above. Positive values indicate that an integration package raises RW_{pew} or increases $Gini_{RW,pew}$, depending on the outcome considered.

Table 7: Counterfactual Results: Combined Effects of Domestic and External Frictions

	Case 0	**Case 1C**	**Case 2C**	**Case 3C**
Set to 1997	None	Dom. MCTC & Ext. TC	Dom. MC & Ext. TC	Dom. TC & Ext. TC
RW_{pew}	1.0000	0.8711	0.9485	0.8842
$Gini_{RW,pew}$	1.0000	0.9608	0.9935	0.9460
	Case X	**Case 1CX**	**Case 2CX**	**Case 3CX**
Set to 1997	Age dist.	Age dist. & Dom. MCTC & Ext. TC	Age dist. & Dom. MC & Ext. TC	Age dist. & Dom. TC & Ext. TC
RW_{pew}	1.0046	0.8744	0.9539	0.8868
$Gini_{RW,pew}$	0.9913	0.9562	0.9811	0.9422

Notes: All entries are normalized by Case 0. Each counterfactual sets the listed fundamentals to their 1997 calibrated values and keeps all other fundamentals at the 2017 benchmark. The upper block keeps the 2017 age distribution and changes only the listed friction blocks to their 1997 values. The lower block repeats the same exercises but also sets the age distribution to its 1997 value. "Age dist." denotes the population age distribution. "Dom. MC" denotes domestic migration costs, "Dom. TC" denotes domestic trade costs, "Dom. MCTC" denotes domestic migration costs and domestic trade costs jointly, and "Ext. TC" denotes external trade costs. $RW_{pew} = \sum_n W_n L^e_n / P_n / \sum_n L^e_n$ is aggregate real wage income per effective worker. $Gini_{RW,pew}$ is the Gini coefficient of W_n/P_n across Chinese regions.

Under the 2017 age structure, the full package of lower domestic migration costs, domestic trade costs, and China–ROW trade costs raises RW_{pew} by 12.89%. The migration-plus-external package raises RW_{pew} by 5.15%, while the trade-plus-external package raises it by 11.58%. Thus, conditional on external integration, the domestic trade margin is much stronger than the domestic migration margin: the trade-plus-external effect is 2.25 times the migration-plus-external effect. Lower trade costs improve market access and reduce intermediate-input costs, so goods-flow channels account for most aggregate real-wage gains.

The lower panel of Table 7 shows how these effects change under the younger 1997 age structure. The full-package gain is 12.89% under the 2017 age structure and 12.96% under the 1997 age structure, so ageing slightly reduces the effect by 0.5%. For the migration-plus-external package, ageing raises the gain from 5.05% to 5.15%, a relative increase of 2.0%. For the trade-plus-external package, ageing lowers the gain from 11.73% to 11.58%, a relative decline of 1.2%. Hence, ageing makes the migration-plus-external force more valuable for aggregate real wages, but slightly dampens the gains from packages in which the goods-flow margin is dominant.

The distributional ranking is different. Under the 2017 age structure, the full package raises $Gini_{RW,pew}$ by 3.92%. The migration-plus-external package raises it by only 0.65%, while the trade-plus-external package raises it by 5.40%. Thus, the trade-plus-external package generates the largest increase in spatial dispersion. External integration benefits regions unevenly because provinces differ in foreign-market exposure and imported-input use, and domestic trade integration reinforces this goods-market channel. Domestic migration integration partly offsets this concentration when all three frictions decline together, so the full package raises the Gini less than the trade-plus-external package.

Ageing also changes how these integration packages affect spatial inequality. Under the 1997 age structure, the full package raises $Gini_{RW,pew}$ by 3.54%; under the 2017 age structure, the effect rises to 3.92%, a relative increase of 10.7%. For the migration-plus-external package, ageing reduces the dispersion effect from 1.03% to 0.65%. For the trade-plus-external package, ageing raises the dispersion effect from 4.95% to 5.40%. Thus, ageing amplifies the inequality effect of packages in which goods-market integration dominates, but dampens the inequality effect of the migration-plus-external package.

Summary In sum, the aggregate gains from integration mainly come through goods flows. Domestic trade integration raises RW_{pew} by 7.82 percent, compared with 2.44 percent from domestic migration integration and 3.13 percent from external integration. When domestic and external forces are combined, the trade-plus-external package generates much larger real-wage gains than the migration-plus-external package.

Ageing changes these effects mainly through age-specific labor reallocation. It raises the real-wage gain from lower migration costs, while slightly reducing the gains from lower domestic and external trade costs. The distributional effects differ: domestic migration integration is the strongest equalizing force, while external and trade-plus-external integration raise spatial dispersion. We next turn to the provincial effects behind these aggregate patterns.

5.3 Provincial Effects and Spatial Reallocation

This subsection examines the provincial effects of population ageing, domestic migration frictions, internal trade frictions, and external trade frictions. The outcome of interest is real wage income per effective worker across Chinese provinces.

Domestic and External Frictions We first decompose the provincial effects of the four forces of interest. The 2017 economy is used as the normalized benchmark, and each counterfactual resets one block of fundamentals to its calibrated 1997 level. Figure 4 reports the resulting changes in provincial real wage income per effective worker when we reset inter-

Figure 4: The Decomposition of Regional Welfare Effects

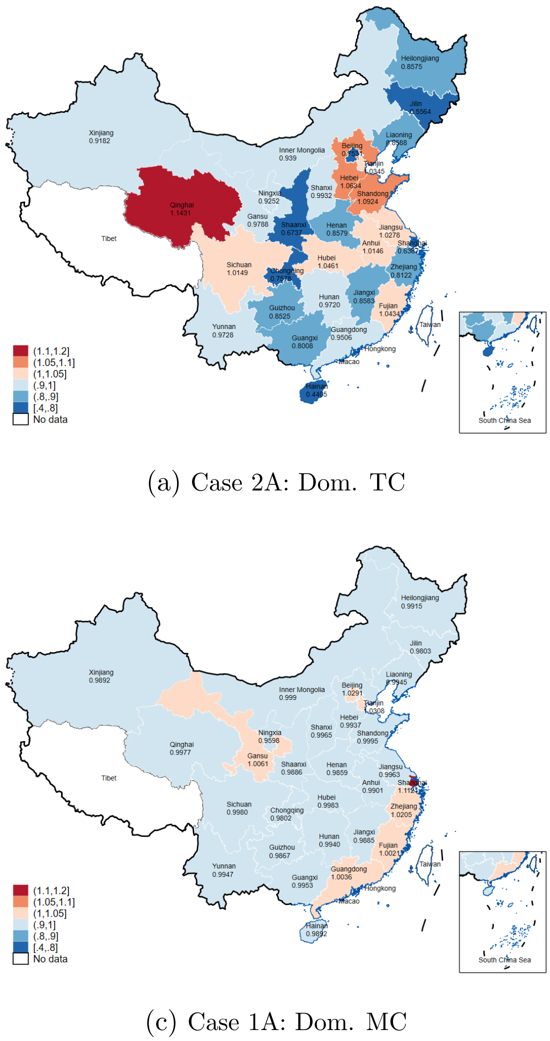

(a) Case 2A: Dom. TC

(b) Case 2B: Ext. TC

(c) Case 1A: Dom. MC

(d) Case X: Age dist.

Notes: All entries are normalized by Case 0. Each counterfactual resets the listed fundamental to its 1997 calibrated value, keeping all other fundamentals at the 2017 benchmark. "Age dist." denotes the population age distribution. "Dom. MC", "Dom. TC", and "Ext. TC" denote domestic migration costs, domestic trade costs, and external trade costs, respectively. The reported measure $RW_{pew} = \sum_n W_n L_n^e / P_n / \sum_n L_n^e$ is aggregate real wage income per effective worker.

nal trade costs, China–ROW trade costs, domestic migration costs, and the population age structure, respectively. Because these exercises reset 2017 fundamentals to their 1997 values, they should be interpreted as historical reversals of integration or demographic change. A value below one indicates that removing the corresponding 1997–2017 change lowers provincial real wage income relative to the 2017 benchmark, while a value above one reflects the general-equilibrium redistribution induced by the counterfactual reversal.

The upper-left panel shows how provincial real wage income responds when internal trade costs are reset from their 2017 levels to their higher 1997 levels. The effects are highly heterogeneous across provinces. Qinghai records the largest increase, followed by Shandong, Hebei, and Sichuan. These results suggest that lower internal trade costs reallocate income away from some relatively less advantaged regions toward provinces with stronger market access, higher productivity, or greater comparative advantage in interregional trade. By contrast, Hainan, Shanghai, Beijing, Chongqing, and Jilin record lower real wage income when internal trade integration is reversed. These provinces benefit more from lower internal trade costs, consistent with their stronger economic fundamentals and greater ability to exploit domestic market integration.

The upper-right panel illustrates the provincial effects of resetting China–ROW trade costs to their 1997 levels. Most provinces experience declines in real wage income when external integration is reversed, with Shanghai showing the largest loss. This pattern is consistent with Shanghai's role as one of China's most open and internationally connected regions. At the same time, some less externally oriented provinces, such as Qinghai, Inner Mongolia, and Heilongjiang, record higher real wage income under higher external trade costs. This does not imply that higher external trade barriers are welfare improving in the aggregate. Rather, it reflects the spatial redistribution generated by external integration, which tends to favor provinces more directly connected to international markets.

The lower-left panel reports the provincial effects of resetting domestic migration costs to their 1997 levels. Higher migration frictions reduce real wage income in many provinces because they restrict the reallocation of workers toward regions with higher real payoffs. However, several coastal and developed provinces, including Shanghai, Zhejiang, Fujian, and Guangdong, exhibit higher real wage income under higher migration costs. This pattern reflects a local labor-supply channel. When migration frictions are higher, inflows into these destination provinces are smaller, which reduces local labor-market competition and can raise real wage income per effective worker for incumbent workers. This provincial effect should be interpreted as a distributional consequence of restricted migration rather than as an aggregate welfare gain from higher migration frictions.

Finally, the lower-right panel shows how resetting the population age structure to its younger 1997 distribution affects provincial real wage income. Most provinces experience modest increases in real wage income, consistent with the aggregate result that the younger 1997 age structure raises real wage income per effective worker. The magnitude is relatively small because the exercise holds aggregate population fixed and changes only the age composition. The effects are nevertheless spatially uneven. In regions that entered the ageing process earlier or had distinctive migration patterns, such as Shanghai, Beijing, and the northeastern provinces, real wage income per effective worker declines under the 1997 age structure. This indicates that demographic change affects provincial outcomes not only through the aggregate supply of effective labor, but also through the spatial reallocation of workers across age groups.

Frictions with the 1997 Age Structure We next examine how population age structure interacts with domestic and external frictions in shaping provincial real wage income per effective worker. Specifically, we allow the population age distribution to change jointly with domestic migration costs, internal trade costs, external trade costs, or all three frictions. Figure 5 reports the results.

The top two panels show that changes in the population age structure modify the provincial effects of internal and external trade-cost changes. Comparing Figure 5 with Figure 4, the interaction with age structure is modest for internal trade costs but more visible for external trade costs in some provinces. For example, Qinghai's relative real wage income under the internal-trade-cost counterfactual increases from 1.1431 without the age-structure change to 1.1436 when the age structure is also reset to its 1997 distribution. By contrast, Shanghai's relative real wage income under the external-trade-cost counterfactual declines from 0.8755 to 0.8530 when the age structure is reset simultaneously. These patterns suggest that demographic composition can reinforce the spatial consequences of trade integration, especially in provinces whose gains are closely tied to external market access and comparative advantage. However, the aggregate implications for real income and regional inequality depend on the full distribution of provincial effects and on the initial economic weights of different regions. The spatial pattern can therefore differ from the aggregate effects reported above.

The bottom-left panel reports the joint effect of resetting the population age structure and domestic migration costs to their 1997 levels. Compared with the migration-cost counterfactual in Figure 4, the additional age-structure change weakens the positive real-wage effects for several developed coastal provinces. For instance, Shanghai's relative real wage income falls from 1.1121 to 1.0606, and Guangdong changes from a small gain of 1.0036 to a slight loss. This pattern indicates that the younger 1997 age structure offsets part of the real-wage gains that developed coastal regions obtain from higher migration frictions. By reducing the relative advantage of these destination provinces, the age-structure change also helps mitigate the increase in regional income disparity. This is consistent with the change

Figure 5: The Welfare Effects of Age Distribution and Frictions

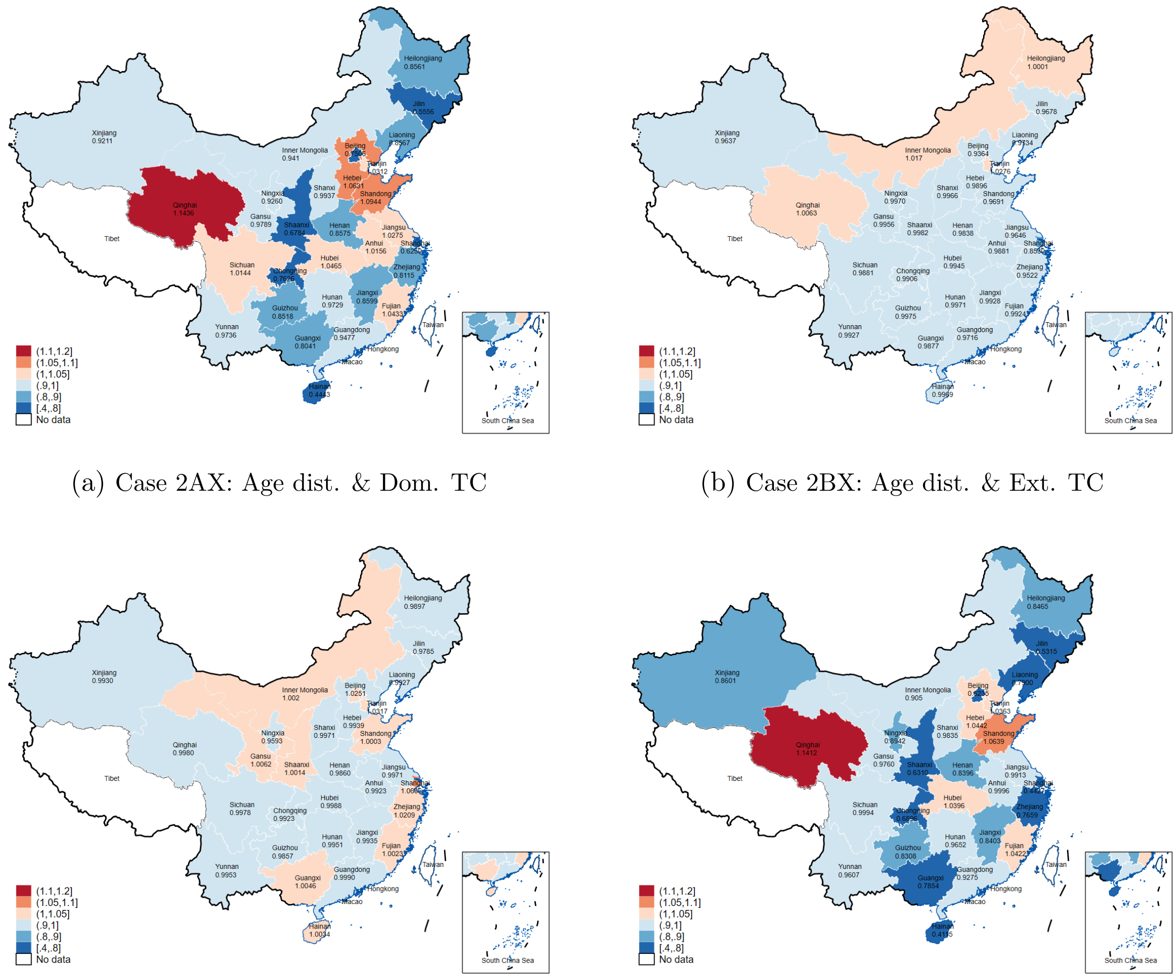

(a) Case 2AX: Age dist. & Dom. TC

(b) Case 2BX: Age dist. & Ext. TC

(c) Case 1AX: Age dist. & Dom. MC

(d) Case 1CX: Age dist. & Dom. MCTC & Ext. TC

Notes: All entries are normalized by Case 0. Each counterfactual resets the listed fundamentals to their 1997 values, keeping the rest at the 2017 benchmark. The upper block uses the 2017 age distribution; the lower block also resets the age distribution to 1997. "Age dist." denotes population age distribution; "Dom. MC", "Dom. TC", "Dom. MCTC", and "Ext. TC" denote domestic migration costs, domestic trade costs, domestic migration and trade costs jointly, and external trade costs. $RW_{pew} = \sum_n W_n L_n^e / P_n / \sum_n L_n^e$ is aggregate real wage income per effective worker.

from Case 1A to Case 1AX in Table 6, where the joint age-structure adjustment is associated with a lower Gini coefficient and a higher aggregate real-income effect.

The bottom-right panel presents the combined effects of resetting all four driving forces to their 1997 levels: population age structure, domestic migration costs, internal trade costs, and external trade costs. The resulting provincial pattern is broadly similar to the scenario in which only internal trade costs are reset. This similarity is consistent with Figure 4, which shows that internal trade costs generate the largest provincial real-wage effects among the four forces. The other three forces still matter, but their provincial impacts are smaller and therefore do not substantially overturn the spatial pattern driven by internal trade integration.

Summary Taken together, the provincial results show that domestic integration, external integration, and population ageing reshape regional real wage income through different spatial channels. Internal trade integration generates the largest provincial reallocation, while external integration mainly benefits provinces more closely connected to international markets. Migration integration raises aggregate real wage income, but its provincial effects are distributional: destination provinces may experience lower real wage income per effective worker when migration inflows increase, whereas other regions benefit from improved labor reallocation. Population ageing further modifies these patterns. Its interaction with trade-cost changes reinforces the role of market access and comparative advantage in some provinces, while its interaction with migration-cost changes weakens the relative gains of developed coastal destinations and helps reduce regional inequality. These results indicate that demographic structure is not only an independent determinant of regional welfare, but also a state variable that shapes how domestic and external integration affect the spatial distribution of income.

6 Conclusion

The main contribution of this paper is to quantify how population ageing changes the regional gains from domestic and external integration in China. To answer this question, we develop a multi-region, multi-sector Ricardian trade model with age-specific labor mobility. Chinese regions are linked through internal migration, interregional trade, and trade with the rest of the world, while workers differ by age in labor efficiency, migration elasticities, and migration frictions. We calibrate the model to Chinese provincial data and use it to study how the 1997–2017 changes in age structure, domestic migration costs, internal trade costs, and China–ROW trade costs shape aggregate real wages and their spatial distribution.

The results can be summarized along four dimensions. First, ageing lowers aggregate real wage income per effective worker and raises regional real-wage inequality when aggregate population is held fixed. Second, aggregate gains from integration mainly come from goods flows: domestic trade integration generates larger real-wage gains than migration or external integration, and this dominance remains when internal and external trade costs fall jointly.

Third, ageing reshapes these gains through age-specific labor reallocation. It raises the real-wage gain from lower migration costs, while slightly reducing the gains from lower internal and external trade costs. Fourth, the provincial results show that these forces operate through different spatial channels: internal trade integration generates the largest provincial reallocation, external integration favors provinces more connected to world markets, and migration integration has distributional effects across regions. Overall, trade integration drives most aggregate gains, while ageing shapes their spatial distribution.

The counterfactuals also clarify the mechanisms behind these results. Lower trade costs improve market access, reduce intermediate-input costs, and shift production across provinces. Lower migration costs reallocate workers toward regions with higher real payoffs, but the strength of this response depends on age composition. In an older economy, migration responses are weaker and migration frictions become more binding, so reducing these frictions has a larger marginal value. The provincial results show the spatial counterpart: external integration favors internationally connected provinces, while migration inflows can reduce real wage income per effective worker in developed destination provinces through local labor-supply effects. Population ageing further modifies these patterns by reinforcing market-access differences under trade-cost changes and weakening the relative gains of developed coastal destinations under migration-cost changes.

Several extensions would be natural next steps. First, adding capital accumulation would allow migration, production costs, and regional investment to adjust jointly, clarifying how ageing affects capital allocation and local adjustment. Second, while our model treats regional and China–ROW trade imbalances as exogenous transfers, making them endogenous could link demographic change and integration to saving, expenditure, and capital flows. Third, introducing uncertainty would allow workers and firms to respond to stochastic demographic, productivity, migration-cost, or trade-cost shocks. We leave these and related extensions for future research.

References

Ahlfeldt, Gabriel M., Stephen J. Redding, Daniel M. Sturm, and Nikolaus Wolf. 2015. "The Economics of Density: Evidence from the Berlin Wall." *Econometrica* 83 (6):2127–2189.

Allen, Treb and Costas Arkolakis. 2014. "Trade and the Topography of the Spatial Economy." *Quarterly Journal of Economics* 129 (3):1085–1140.

Amiti, Mary, Mi Dai, Robert C. Feenstra, and John Romalis. 2020. "How Did China's WTO Entry Affect U.S. Prices?" *Journal of International Economics* 126:103339.

Autor, David H., David Dorn, and Gordon H. Hanson. 2013. "The China Syndrome: Local Labor Market Effects of Import Competition in the United States." *American Economic Review* 103 (6):2121–2168.

Boustan, Leah Platt, Matthew E. Kahn, Paul W. Rhode, and Maria Lucia Yanguas. 2020. "The Effect of Natural Disasters on Economic Activity in US Counties: A Century of Data." *Journal of Urban Economics* 118:103257.

Brandt, Loren and Kevin Lim. 2024. "Opening up in the 21st Century: A Quantitative Accounting of Chinese Export Growth." *Journal of International Economics* 150:103895.

Brandt, Loren, Johannes Van Biesebroeck, and Yifan Zhang. 2012. "Creative Accounting or Creative Destruction? Firm-Level Productivity Growth in Chinese Manufacturing." *Journal of Development Economics* 97 (2):339–351.

Broda, Christian and David E. Weinstein. 2006. "Globalization and the Gains from Variety." *Quarterly Journal of Economics* 121 (2):541–585.

Caliendo, Lorenzo, Maximiliano Dvorkin, and Fernando Parro. 2019. "Trade and Labor Market Dynamics: General Equilibrium Analysis of the China Trade Shock." *Econometrica* 87 (3):741–835.

Caliendo, Lorenzo and Fernando Parro. 2015. "Estimates of the Trade and Welfare Effects of NAFTA." *Review of Economic Studies* 82 (1):1–44.

Caliendo, Lorenzo, Fernando Parro, Esteban Rossi-Hansberg, and Pierre-Daniel Sarte. 2018. "The Impact of Regional and Sectoral Productivity Changes on the U.S. Economy." *Review of Economic Studies* 85 (4):2042–2096.

Department of Population and Employment Statistics, National Bureau of Statistics of China. 2016. *2015 nian quanguo 1% renkou chouyang diaocha ziliao*. Beijing: China Statistics Press. In Chinese: 20151%.

Eaton, Jonathan and Samuel Kortum. 2002. "Technology, Geography, and Trade." *Econometrica* 70 (5):1741–1779.

Feenstra, Robert C., Robert Inklaar, and Marcel P. Timmer. 2015. "The Next Generation of the Penn World Table." *American Economic Review* 105 (10):3150–3182.

Giannone, Elisa et al. 2024. "Living in a Ghost Town: The Geography of Depopulation and Aging." Working paper.

Greenland, Andrew, John Lopresti, and Peter McHenry. 2019. "Import Competition and Internal Migration." *Review of Economics and Statistics* 101 (1):44–59.

Groningen Growth and Development Centre. 2021. "Penn World Table Version 10.0." Dataset. University of Groningen.

Handley, Kyle and Nuno Limão. 2017. "Policy Uncertainty, Trade, and Welfare: Theory and Evidence for China and the United States." *American Economic Review* 107 (9):2731–2783.

Hsieh, Chang-Tai and Ralph Ossa. 2016. "A Global View of Productivity Growth in China." *Journal of International Economics* 102:209–224.

Karahan, Fatih and Serena Rhee. 2017. "Population Aging, Migration Spillovers, and the Decline in Interstate Migration." Staff Report 699, Federal Reserve Bank of New York. Revised version.

Monte, Ferdinando, Stephen J. Redding, and Esteban Rossi-Hansberg. 2018. "Commuting, Migration, and Local Employment Elasticities." *American Economic Review* 108 (12):3855–3890.

National Bureau of Statistics of China. 2007. "China 2005 1% Population Survey Data Assembly." CD-ROM; bilingual English and Chinese edition.

OECD. 2021. "Inter-Country Input-Output Tables." Dataset. OECD ICIO database.

Pierce, Justin R. and Peter K. Schott. 2016. "The Surprisingly Swift Decline of U.S. Manufacturing Employment." *American Economic Review* 106 (7):1632–1662.

Poncet, Sandra. 2003. "Measuring Chinese Domestic and International Integration." *China Economic Review* 14 (1):1–21.

Redding, Stephen J. 2016. "Goods Trade, Factor Mobility and Welfare." *Journal of International Economics* 101:148–167.

Redding, Stephen J. and Esteban Rossi-Hansberg. 2017. "Quantitative Spatial Economics." *Annual Review of Economics* 9 (1):21–58.

Simonovska, Ina and Michael E. Waugh. 2014. "The Elasticity of Trade: Estimates and Evidence." *Journal of International Economics* 92 (1):34–50.

Sposi, Michael, Kei-Mu Yi, and Jing Zhang. 2025. "Premature Deindustrialization and Industry Polarization." NBER Working Paper 29483, National Bureau of Economic Research. Revised September 2025.

Suzuki, Yuta. 2023. "Local Shocks and Regional Dynamics in an Aging Economy." Working paper.

Tombe, Trevor and Xiaodong Zhu. 2019. "Trade, Migration, and Productivity: A Quantitative Analysis of China." *American Economic Review* 109 (5):1843–1872.

Yamano, Norihiko, Joaquim Guilhoto, Ali Alsamawi, Colin Webb, Peter Horvát, Agnès Cimper, Carmen Zürcher, and Xue Han. 2021. "Development of the OECD Inter-Country Input-Output Database 2021." OECD Science, Technology and Industry Working Papers 2021/14, OECD Publishing.

Young, Alwyn. 2000. "The Razor's Edge: Distortions and Incremental Reform in the People's Republic of China." *Quarterly Journal of Economics* 115 (4):1091–1135.

Yu, Miaojie. 2015. "Processing Trade, Tariff Reductions and Firm Productivity: Evidence from Chinese Firms." *The Economic Journal* 125 (585):943–988.

Zhao, Q., C. Pan, Z. Zhang, X. C. Guo et al. 2024. "An Inter-Regional Input-Output Table Series of China from 1987–2017 with Integrated Carbon Emission Data." *Scientific Data* 11 (1):1335.

Zheng, Heran, Zengkai Zhang, Wendong Wei, Malin Song, Erik Dietzenbacher, Xingyu Wang, Jing Meng, Yuli Shan, Jiamin Ou, and Dabo Guan. 2021. "Chinese Provincial Multi-Regional Input-Output Database for 2012, 2015, and 2017." *Scientific Data* 8 (1):244.

Appendix

A Model Details

Table A.1: Equilibrium Conditions

ID	Level equation	Scope
H1	$\bar{L}_{n,g} = (1-\phi_{n,g})N_{n,g}, \qquad \bar{L}^e_{n,g} = l^g \bar{L}_{n,g}$	$\forall(n,g)$
H2	$\bar{L}_n = \sum_{g\in\mathcal{G}^W} \bar{L}_{n,g}, \qquad \bar{L}^e_n = \sum_{g\in\mathcal{G}^W} \bar{L}^e_{n,g}$	$\forall n$
H3	$\chi_{n,g} = -\varphi_n W_n l^g + T l^g, \qquad T = \dfrac{\sum_{n=1}^N \varphi_n W_n L^e_n}{\sum_{n=1}^N L^e_n}$	$\forall(n,g)$
H4	$\Lambda_{n,g} = \dfrac{W_n l^g + \chi_{n,g}}{P_n}$	$\forall(n,g)$
H5	$\mu_{nm,g} = \dfrac{\left(\Lambda_{n,g}/\nu_{nm,g}\right)^{\kappa^g}}{\sum_{i\in\mathbb{N}_0}\left(\Lambda_{i,g}/\nu_{im,g}\right)^{\kappa^g}}$	$\forall(n,m,g)$
H6	$L_{n,g} = \sum_{m\in\mathbb{N}_0} \mu_{nm,g}\bar{L}_{m,g}, \qquad L^e_{n,g} = l^g L_{n,g}$	$\forall(n,g)$
H7	$L_n = \sum_{g\in\mathcal{G}^W} L_{n,g}, \qquad L^e_n = \sum_{g\in\mathcal{G}^W} L^e_{n,g}$	$\forall n$
P1	$c^j_n = \Upsilon^j_n W_n^{\gamma^j_n} \prod_{k=1}^J (P^k_n)^{\gamma^{jk}_n}, \qquad \Upsilon^j_n = (\gamma^j_n)^{-\gamma^j_n} \prod_{k=1}^J (\gamma^{jk}_n)^{-\gamma^{jk}_n}$	$\forall(n,j)$
P2	$P^j_n = A^j \left[\sum_{i=1}^N \lambda^j_i (\kappa^j_{ni} c^j_i)^{-\theta}\right]^{-1/\theta}, \qquad A^j = \left[\Gamma\left(\frac{1+\theta-\sigma^j}{\theta}\right)\right]^{\frac{1}{1-\sigma^j}}$	$\forall(n,j)$
P3	$\pi^j_{ni} = \dfrac{\lambda^j_i (c^j_i \kappa^j_{ni})^{-\theta}}{\sum_{m=1}^N \lambda^j_m (c^j_m \kappa^j_{nm})^{-\theta}}$	$\forall(n,i,j)$
A1	$P_n = \prod_{j=1}^J \left(\dfrac{P^j_n}{\alpha^j_n}\right)^{\alpha^j_n}, \qquad P^j_n c^j_{n,g} = \alpha^j_n P_n c_{n,g}$	$\forall(n,j,g)$
A2	$C_n = \sum_{g\in\mathcal{G}^W} c_{n,g} L_{n,g}, \qquad C^j_n = \sum_{g\in\mathcal{G}^W} c^j_{n,g} L_{n,g}$	$\forall(n,j)$
A3	$P^j_n C^j_n = \alpha^j_n P_n C_n$	$\forall(n,j)$
A4	$D_n = \sum_{g\in\mathcal{G}^W} \chi_{n,g} L_{n,g} = -\varphi_n W_n L^e_n + T L^e_n$	$\forall n$
A5	$P_n C_n = W_n L^e_n + D_n$	$\forall n$
A6	$X^j_n = P^j_n Q^j_n = P^j_n C^j_n + \sum_{k=1}^J \gamma^{kj}_n Y^k_n = \alpha^j_n P_n C_n + \sum_{k=1}^J \gamma^{kj}_n Y^k_n$	$\forall(n,j)$
A7	$Y^j_n = \sum_{i=1}^N \pi^j_{in} X^j_i$	$\forall(n,j)$
A8	$W_n L^e_n = \sum_{j=1}^J \gamma^j_n Y^j_n$	$\forall n$

B Calibration Details

B.1 Regions

Table B.1: Mainland Chinese Province-Level Administrative Regions

Code	Region	Code	Region	Code	Region	Code	Region
11	Beijing	31	Shanghai	42	Hubei	53	Yunnan
12	Tianjin	32	Jiangsu	43	Hunan	61	Shaanxi
13	Hebei	33	Zhejiang	44	Guangdong	62	Gansu
14	Shanxi	34	Anhui	45	Guangxi	63	Qinghai
15	Inner Mongolia	35	Fujian	46	Hainan	64	Ningxia
21	Liaoning	36	Jiangxi	50	Chongqing	65	Xinjiang
22	Jilin	37	Shandong	51	Sichuan		
23	Heilongjiang	41	Henan	52	Guizhou		

Notes: The table reports the 30 mainland Chinese province-level administrative regions used in the benchmark calibration, excluding Tibet.

B.2 Sectoral Gross-Output Prices

The price series used in the trade block are sectoral gross-output prices, while the available price data are value-added prices. We therefore use the production structure to convert value-added prices into gross-output prices, following the approach in Sposi, Yi, and Zhang (2025).

Sector j in region n produces with value added and intermediate inputs according to

$$y_n^j(\omega) = q_n^j(\omega) \left(\ell_n^j(\omega)\right)^{\gamma_n^j} \prod_{k=1}^{J} \left(m_n^{jk}(\omega)\right)^{\gamma_n^{jk}}, \tag{B.1}$$

where γ_n^j is the value-added share in sector j, and γ_n^{jk} is the cost share of sector-k intermediate inputs in sector-j production. Thus, j indexes the output sector and k indexes the input sector.

Let $p_{n,t}^{v,j}$ denote the value-added price of sector j in region n at time t, and let $P_{n,t}^j$ denote the corresponding gross-output price. Cost minimization implies

$$\ln P_{n,t}^j = \gamma_{n,t}^j \ln p_{n,t}^{v,j} + \sum_{k=1}^{J} \gamma_{n,t}^{jk} \ln P_{n,t}^k - \gamma_{n,t}^j \ln \gamma_{n,t}^j - \sum_{k=1}^{J} \gamma_{n,t}^{jk} \ln \gamma_{n,t}^{jk}. \tag{B.2}$$

Stacking the three sectoral equations gives

$$\ln \mathbf{P}_{n,t} = \left(\mathbf{I}_3 - \mathbf{\Gamma}_{n,t}\right)^{-1} \left(\mathbf{p}^v_{n,t} - \mathbf{c}_{n,t}\right), \tag{B.3}$$

where

$$\ln \mathbf{P}_{n,t} \equiv \begin{bmatrix} \ln P^1_{n,t} \\ \ln P^2_{n,t} \\ \ln P^3_{n,t} \end{bmatrix}, \qquad \mathbf{p}^v_{n,t} \equiv \begin{bmatrix} \gamma^1_{n,t} \ln p^{v,1}_{n,t} \\ \gamma^2_{n,t} \ln p^{v,2}_{n,t} \\ \gamma^3_{n,t} \ln p^{v,3}_{n,t} \end{bmatrix}, \tag{B.4}$$

$$\mathbf{I}_3 \equiv \begin{bmatrix} 1 & 0 & 0 \\ 0 & 1 & 0 \\ 0 & 0 & 1 \end{bmatrix}, \qquad \mathbf{\Gamma}_{n,t} \equiv \begin{bmatrix} \gamma^{11}_{n,t} & \gamma^{12}_{n,t} & \gamma^{13}_{n,t} \\ \gamma^{21}_{n,t} & \gamma^{22}_{n,t} & \gamma^{23}_{n,t} \\ \gamma^{31}_{n,t} & \gamma^{32}_{n,t} & \gamma^{33}_{n,t} \end{bmatrix}, \tag{B.5}$$

and

$$\mathbf{c}_{n,t} \equiv \begin{bmatrix} \gamma^1_{n,t} \ln \gamma^1_{n,t} + \sum_{k=1}^{3} \gamma^{1k}_{n,t} \ln \gamma^{1k}_{n,t} \\ \gamma^2_{n,t} \ln \gamma^2_{n,t} + \sum_{k=1}^{3} \gamma^{2k}_{n,t} \ln \gamma^{2k}_{n,t} \\ \gamma^3_{n,t} \ln \gamma^3_{n,t} + \sum_{k=1}^{3} \gamma^{3k}_{n,t} \ln \gamma^{3k}_{n,t} \end{bmatrix}. \tag{B.6}$$

Solving equation (B.3) gives the sectoral gross-output prices $P^j_{n,t}$.